DEVELOPMENT OF AEROGEL FIBERS AND COMPOSITES FOR TEXTILES

by

Faheem Ahmad

A Dissertation Submitted to the
Graduate School of Sciences and Engineering
in Partial Fulfillment of the Requirements for
the Degree of

Doctor of Philosophy

in

Materials Science and Engineering

KOÇ ÜNİVERSİTESİ

January 8, 2020

DEVELOPMENT OF AEROGEL FIBERS AND COMPOSITES FOR TEXTILES

Koç University

Graduate School of Sciences and Engineering

This is to certify that I have examined this copy of a doctoral dissertation by

Faheem Ahmad

and have found that it is complete and satisfactory in all respects,
and that any and all revisions required by the final
examining committee have been made.

Committee Members:

Prof. Can Erkey (Advisor)

Assoc. Prof. Uğur Ünal

Assoc. Prof. Seda kızılel

Assist. Prof. Zeynep Ülker

Assist. Prof. Yaprak Ozbakir

Date: _____

To my grandmother (late) who left this world for heaven during my PhD studies

ABSTRACT

DEVELOPMENT OF AEROGEL FIBERS AND COMPOSITES FOR TEXTILES

Faheem Ahmad

Doctor of Philosophy in Materials Science and Engineering

January 2020

Aerogels are a class of nanostructured materials with some extraordinary properties like low densities, high porosities, high surface areas and low thermal conductivities. These properties of aerogels make them very attractive as fabrics for thermal insulation, liquid absorption, sound absorption and medical textiles. In this work, pure aerogel fibers and aerogel based nonwoven fibrous composites were prepared. A composite of alginate aerogel with polyester (PET) nonwoven was synthesized by a sol-gel method. A needle punched PET nonwoven was soaked with an alginate solution and then immersed in an aqueous $CaCl_2$ solution which resulted in the formation of a gel inside the PET nonwoven. The gel was dried with supercritical CO_2 after solvent exchange with ethanol leading to alginate aerogel-PET nonwoven composite. The aerogels were porous and were in the form of blocks in between the PET fibers as evident from SEM images. The thermal properties of the composite were measured using a heat flow meter. The thermal diffusivity of the composite was significantly lower than the thermal diffusivity of the pure PET nonwoven. The composite also had a higher thermal resistance and a higher tensile strength than the pure PET nonwoven. Experiments using a thermal imaging camera indicated that the heat flux in the composite is much lower than in pure PET nonwoven due to the presence of alginate aerogel. The results show that the new composite material is promising for use in thermal clothing applications.

A composite of cellulose aerogel with needle punched cotton nonwoven was also synthesized by a sol-gel method. The cotton nonwoven was immersed inside the solution of cellulose and heated at 50 ºC for 2 hours which led to the formation of layers of gel inside the cotton nonwoven. Then gel was dried with supercritical CO_2 after solvent exchange with acetone to obtain cellulose aerogel cotton nonwoven composite. This composite had a highly porous structure and an average pore diameter of 25 nm. The wound exudate (fluid) absorbency test was performed to determine the performance of this composite for wound dressings. The cellulose aerogel cotton nonwoven composite showed high wound exudate absorbency. Furthermore, silver was loaded inside the aerogel composite in order to achieve antimicrobial properties. The composite was soaked in 0.02 M solution of silver nitrate after solvent exchange with acetone and dried supercritically. The composite exhibited excellent antibacterial resistance against Escherichia coli bacteria.

The pure aerogel fibers were produced from sodium alginate. Firstly, alginate gel fibers were synthesized by extrusion of an alginate solution (three different concentrations in water) into a $CaCl_2$ aqueous solution using a syringe pump. Removal of water from the gel fibers by solvent exchange with ethanol followed by supercritical extraction of ethanol at 308 K and 10 MPa resulted in alginate aerogel fibers. Three different kinds of alginate aerogel fibers were prepared by changing the concentration of the alginate solution. The aerogel fibers were characterized by mercury porosimetery, scanning electron microscopy, Raman spectroscopy and tensile strength tester. All three fibers were highly porous with surface areas and densities in the range of 220 m^2/g to 231 m^2/g and 0.2 g/ cm^3 to 0.3 g/ cm^3 respectively. The maximum elongation of the fibers ranged from 12 % to 15 % while their elastic modulus ranged from 0.26 MPa to 0.45 MPa.

ÖZET

Aerojeller, düşük yoğunluğa, yüksek gözenekliliğe, düşük ısı iletkenliğine ve yüksek yüzey alanına sahip bir nanoyapılı malzeme sınıfıdır. Aerojellerin bu özellikleri, onların ısı yalıtımında, sıvı ve ses emiliminde ve tıbbi tekstil malzemelerinde kullanımını çekici kılmaktadır. Bu çalışmada, saf aerojel elyaflar ve aerojel bazlı dokunmamış elyaflı kompozitler hazırlandı. Aljinat aerojel ve dokunmamış polyester (PET) kompoziti sol-jel yöntemi ile sentezlendi. Bir iğne ile delinmiş dokunmamış PET, aljinat çözeltisi ile ıslatıldı ve daha sonra sulu bir $CaCl_2$ çözeltisine daldırıldı, bu şekilde dokunmamış PET içerisinde bir jel oluşturuldu. Etanol ile çözücü değişimden sonra, jel süperkiritik CO_2 ile kurutuldu ve aljinat aerojel - dokunmamış PET kompoziti elde edildi. SEM görüntülerinden, aerojellerin gözenekli ve PET elyafları arasında bloklar halinde olduğu görüldü. Kompozitin termal özellikleri bir ısı akış ölçer kullanılarak ölçüldü. Kompozitin termal yayılımı, saf dokunmamış PET malzemenin termal yayılımından önemli ölçüde daha düşüktü. Kompozit, ayrıca saf dokunmamış PET malzemeden daha yüksek bir termal dirence ve daha yüksek bir gerilme mukavemetine sahipti. Bir termal görüntüleme kamerası kullanılarak yapılan deneyler, kompozit içindeki ısı akısının, aljinat aerojelinin varlığı nedeniyle saf dokunmamış PET malzemeye göre çok daha düşük olduğunu gösterdi. Sonuçlar, yeni kompozit malzemenin termal giysi uygulamalarında kullanım için umut verici olduğunu göstermektedir.

İğne ile delinmiş dokunmamış pamuk ve selüloz aerojel kompoziti de bir sol-jel yöntemi ile sentezlendi. Pamuklu dokunmamış malzeme selüloz çözeltisinin içine daldırıldı ve 2 saat boyunca 50 °C'de ısıtıldı. Bu da pamuklu dokunmamış kumaş içinde jel tabakalarının oluşumuna yol açtı. Jel, aseton ile çözücü değişiminden sonra süperkritik CO_2 ile kurutuldu ve jel-selüloz aerojel dokunmamış pamuklu kompoziti elde edildi. Bu kompozit, oldukça gözenekli bir yapıya ve ortalama 25 nm gözenek çapına sahipti. Kompozitin yara bandları için performansını belirlemek üzere yara eksüda (sıvı) emicilik testi yapıldı. Selüloz aerojel- dokunmamış pamuk kompoziti, yüksek yara eksüda emiciliği gösterdi. Antimikrobiyal özelliklere ulaşmak için aerojel kompozitinin içine gümüş yüklendi. Kompozit, aseton ile çözücü değişiminden sonra 0.02 M gümüş nitrat çözeltisine batırıldı ve süperkritik olarak kurutuldu. Kompozit, *Escherichia coli* bakterilerine karşı mükemmel antibakteriyel direnç sergiledi.

Saf aerojel elyaflar sodyum aljinattan üretildi. Aljinat jel elyafları, bir şırınga pompası vasıtasıyla bir aljinat çözeltisinin (su içinde üç farklı konsantrasyon) bir $CaCl_2$ sulu çözeltisine ekstrüzyonu ile sentezlendi. Suyun, jel elyaflardan çözücü değişimi aşamasında etanol ile uzaklaştırılmasının ardından, etanolun 308 K ve 10 MPa'da süperkritik ekstraksiyonu sonucunda aljinat aerojel elyafları elde edildi. Aljinat çözeltisinin konsantrasyonu değiştirilerek üç farklı aljinat aerojel elyafı hazırlandı. Aerojel elyafları, cıva porosimetrisi, taramalı elektron mikroskopisi, Raman spektroskopisi ve gerilme mukavemeti test cihazları ile karakterize edildi. Her üç elyaf

da oldukça gözenekliydi. Yüzey alanları ve yoğunlukları sırasıyla 220 m^2 / g ila 231 m^2 / g ve 0.2 g / cm^3 ila 0.3 g / cm^3 aralığında bulundu. Elyafların maksimum uzaması % 12 ila % 15 arasında değişirken, elastik modülleri 0.26 MPa ila 0.45 MPa arasında değişti.

ACKNOWLEDGMENTS

Firstly, I would like to thank my advisor Prof. Dr. Can Erkey from the cores of my heart for his words of advice and support throughout my PhD studies. He is an inspiration to me and has made a huge impact on my life. He always encouraged and guided me during the whole span of this work.

I wish to thank and acknowledge members of my thesis monitoring committee, Assoc. Prof. Uğur Ünal and Asst. Prof. Zeynep Ülker Demir for their assistance and support.

A special thank to Dr. Selmi Erim Bozbağ, Dr. Yaprak Özbakir, Dr. Barış Yağcı and Dr. Muhammad Anwaar Nazeer for their support and guidance.

I would like to thank my beloved parents M. Siddique Javid and Saeeda Siddique, and my brothers, M. Azeem Ahmad, Aleem Ahmad and Talha Siddique for their love, prayers and support.

A big thank to my wife Sidra Aslam and my daughter Fatima Ahmad for their love and patience.

I also would like to thank my colleagues Muhammad Anas, İbrahim Şahin, Ğohtuğ Gönel, Shadi Khan, Şeçil Ünsal, Umamia Saleem, Zeynep İnönu, Işık Sena, Hande Gunes, Bengisu Baram, Hamed Yousefzadeh and Özge Payanda.

I would like to thank Higher Education Commision (HEC) of Pakistan and Koç University Turkey for their financial and technical support. This research work would not be possible without their support.

TABLE OF CONTENT

LIST OF TABLES

LIST OF FIGURES

NOMENCLATURE

PET	polyethylene terephthalate
MCC	microcrystalline cellulose
TEOS	tetraethyl orthosilicate
$scCO_2$	supercritical carbon dioxide
wt	weight
DNA	deoxyribonucleic acid
RNA	ribonucleic acid

Chapter 1

INTRODUCTION

1.1 Textiles for Thermal Insulation

Textiles are among the necessities of life which provide cover, comfort and protection to the humans. Protection from cold is highly important to maintain the comfort level of human body. Textiles Clothing acts as thermal barrier for human body against the low temperature environment and hinders the flow of heat from body to the surroundings [1]. The thermal insulation, air permeability and water vapor resistance control the comfort properties of textile fabrics. These three parameters mainly depend upon the type of fibers, structure, numbers of layers and chemical treatment of fabric [2]–[4].Woven, knitted and nonwoven fibrous assemblies/structures and clothing are usually used to protect the human body from cold [5]–[7].

Fibers are building block of textile products. The pure natural fibers, synthetic fibers and their blends are commonly used to manufacture different textiles. The physical and mechanical properties of textile fibers are very important to achieve a require output from specific textile product [8]. Textile fibers are firstly spun into yarn and then converted into a fabric by applying weaving or knitting process [9].

Textile fabrics are also produced directly from fibers which are called nonwovens. A fibrous web is usually manufactured by carding, airlaid and wet-laid methods which is later bonded by meanings of the thermal bonding, chemical bonding or mechanical bonding (needles or water jet) to structure nonwoven fabrics.

Thermal bonding deals the formation of nonwoven fabric by employing heat to fibrous web. The fibrous web usually contains a thermoplastic fiber/polymer component which melts to bond the web to form a nonwoven fabric. The nonwoven fabrics produced by thermal bonding are bulker and softer.

The nonwovens are also prepared by incorporating chemical binders to bond the fibers inside the web. The types of binders and fibers influence the strength and stiffness of the fabric. The choice of the binder usually depends upon the applications of nonwoven.

The hydroentanglement bonding is a mechanical process which involves the entanglement of fibers by high speed water jets. These nonwoven fabrics are softer and have compact structure.

The needle punching is a technique in which the fibers are also mechanically entangled by using reciprocating barbed needle. The barbs of needle hold the fibers from moving fibrous web and put them to the perpendicular direction to the fabric. The structure of needle punched nonwoven fabric depends upon the arrangement of fibers during the web formation and web bonding which control the physical and mechanical properties of the fabric. Moreover, the selection of raw material is also important to obtain the desire properties of the fabric. The needle punched nonwovens have shown high porosity and good mechanical properties. The needle punched nonwovens are shown in Figure 1.1 [10].

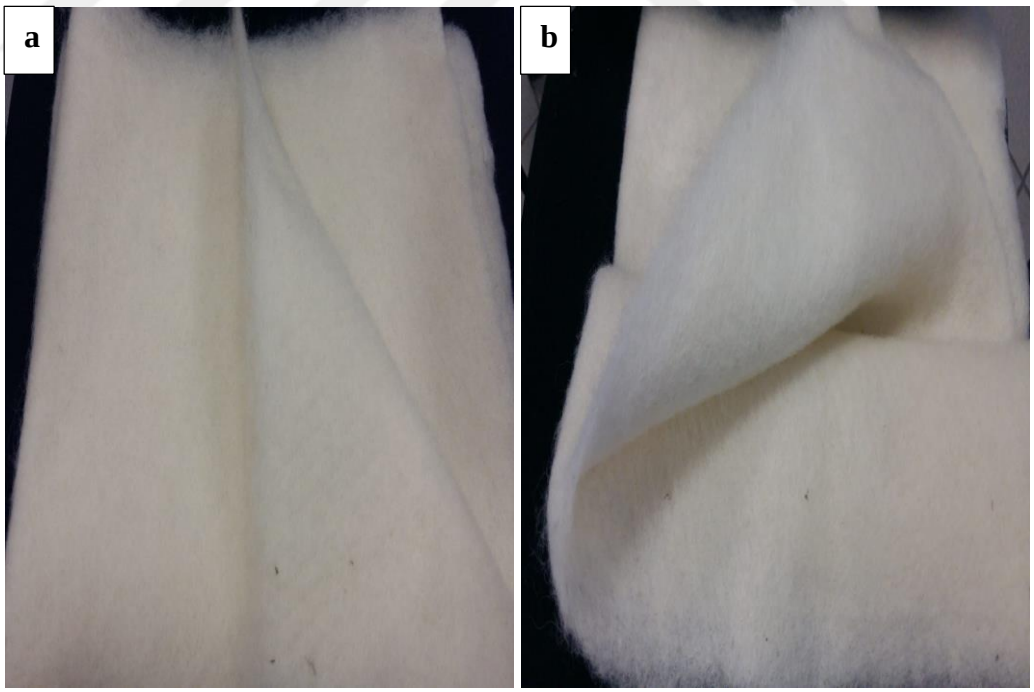

Figure 1.1: (a) Needle punched cotton nonwoven (b) Needle punched wool nonwoven

The nonwovens fibrous assemblies are highly porous, light weight, low density and have low cost of production. Nonwovens are also versatile in terms of usage of raw materials. Moreover, nonwoven fabrics also have high strength, flexibility and good abrasion resistance. Therefore, nonwovens are one of the best available products for insulation applications like blankets. Thermal properties of nonwoven assemblies can be engineered by changing the type of fiber, porosity and the amount of air inside the structure. Porosity of nonwoven is the key to form a thermal barrier because porous structure enables nonwoven to hold air inside it and air has a low thermal conductivity of 0.025 W m^{-1} K^{-1} [11], [12].

The properties of nonwoven can be enhanced by making composites of nonwovens with other types of materials. Such nonwoven composites are prepared by coating or filling the natural or synthetic fibers based nonwovens with different kinds of chemicals such as various resins such as polyvinyl acetate and other various esters. Lots of efforts have been made to develop new nonwoven composites to improve their thermal insulation properties further by varying the combination of raw materials [13], [14].

1.2 Aerogel-based Textile Composite for Thermal Insulation

The aerogels were synthesized by Kistler in 1932 who developed these stable porous materials by removing the pore liquid with gas. Kistler produced several types of aerogels which include silica, tungsten oxide and alumina aerogels. The aerogels were firstly commercialized by Monsanto Chemical Company in 1969 who used silica aerogels as additives for tooth paste, cosmetics and as thickening agents for paints. Afterwards, the organic and hybrid aerogels have also been developed which further spread the areas of application of aerogels. These are available in the forms (Figure 1.2) of beads, monoliths, fibers and composites which are now being used in various applications such as drug delivery, biomedical, food processing, optics, shock absorber, catalysts and energy storage [15]–[18].

Moreover, aerogels are also used for producing materials for thermal insulation due to their nanoporous structure (Figure 1.3) [19], [20]. The total thermal conductivity of these aerogels depends on solid conduction, gas conduction and convection and

thermal radiation contributions. The pore size of aerogels is very low so gas convection is almost negligible [21]. The major contribution of thermal conductivity through these porous aerogels is given by gas conduction which is reduced below air due to the Knudsen effect [22]. As a result, thermal conductivity of aerogels can be as low as 0.01 W m^{-1} K^{-1} [23], [24]. Therefore, silica aerogels have the lowest thermal conductivity among available porous structures and are used for manufacturing of commercially available thermal products [25].

Figure 1.2: (a) Aerogel beads (b) Aerogel monoliths

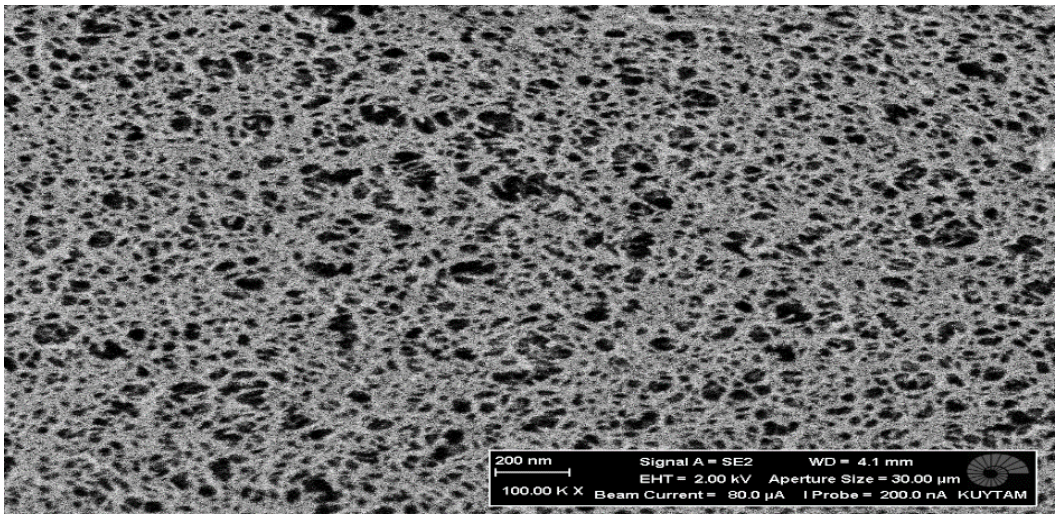

Figure 1.3: SEM image of porous structure of aerogel

Also low density (0.003-0.2g/cm^3) and high surface area (500-1200m^2/g) of silica aerogels have made them attractive for insulation [26]–[28]. However, due to their low densities, these aerogels have highly fragile structure and can crack or disintegrate easily [29].

Silica aerogels are inorganic materials by nature which are mostly prepared by the sol-gel method followed by supercritical drying [30], [31]. Tetraethoxysilane (TEOS), tetramethoxysilane (TMOS) and polyethoxydisiloxane are widely used as a precursor for silica aerogel. Acid or base catalyst is used for hydrolysis of silicon dioxide. The solution of precursor turns into gel by adding it into acid or base catalyst and form a network. This network of this gel contains some unreacted groups like alkoxide groups so to provide strength to this network, aging of gel is done by controlling pH of the solution. It helps to minimize the cracking of solid gel. Water from aging solution is completely removed to prepare it for drying process.

The silica gel is normally dried by using supercritical carbon dioxide drying method. This drying step is most important in context to attain the porous structure of aerogel. The capillary pressure can cause a fracture and can damage the pores of gel. So to avoid this damage, supercritical carbon dioxide removes the liquid (solvent) from the pores of gel above the critical temperature (313 K) and critical pressure (90 bar) which minimize the capillary forces to provide the porous structure of aerogels [32]–[34].

The combination of nonwoven and aerogel in the form of a composite may be one of the most efficient insulating products. These nonwoven composites are made of fibers, resin (aerogel material) and air. The effective thermal conductivity of these composites essentially depends upon the volume fraction of fiber, aerogels and air inside composites [31], [32]. The first aerogel fiberous composite blanket was commercilised in 2000 by Aspen Aerogel. The silica aerogel was incorpoeted into the glasswool fiberous matrix to produce a blanket with high thermal insulation [37].

The silica aerogel blankets are mostly used for insulation of pipes and buildings. NASA has used aerogel blanket as insulation material for Mars Rover and space suits. The aerogels are also used as filler and sandwiched between fabrics to make garments and sleeping bags [17], [38].

Mostly polypropylene, polyester and glass wool nonwoven fibrous structures can be used for these aerogel based composites. These aerogel blankets have thermal conductivity in the range of 0.014 W/m.K and these blankets are also more flexible as compared to pure aerogel [39].

There have been some studies in the literature on preparation of silica aerogel-nonwoven composites. Two general strategies were described to synthesize these composites. The first one is the incorporation of aerogel beads into the nonwoven fibrous web before bonding of the fibers which used to prepare silica aerogel-polyester nonwoven composite. The second technique involves immersing the nonwoven fabric into the solution which later gels inside the fabric. The gel is dried by using supercritical drying method to obtain aerogel based fibrous composite. The silica aerogel-glass fiber composites in the form of blankets are produced by this technique [7], [40], [41].

There have been few studies in literature which investigated the thermal and physical properties of aerogel based nonwoven blanket. These studies concluded that the weight fraction of silica aerogel in the fibrous nonwoven fabric played key role to achieve the required thermal insulation from aerogel incorporated blankets. They also observed that the density of nonwoven fabric and type of textiles fibers are the other important parameters which can change the physical and mechanical properties of aerogel based nonwoven thermal blanket. The blanket fabric made of aerogel fibrous composite is shown in Figure 1.4.

Figure 1.4: Aerogel nonwoven blanket

The use of woven fabrics with blend of two textile fibers is also investigated by the researchers. They incorporated the nanoparticles of silica aerogel in the fabric which was the blend of wool-aramid (65:35) fibers. They observed that the 2 % coating of silica aerogel can increase the thermal resistance of fabric up to 68 % as compared to pure fabric [25], [42], [43].

Silica aerogels have high tendency to produce a lot of dust during their handling. As the silica aerogels are brittle in nature and show limited range of mechanical strength so these aerogels are crushed during bending. The fine dust particles of silica aerogels are oleophilic in nature which results in an unpleasant feeling when using silica aerogel based thermal blankets [29], [39], [44].

A textile remains in contact with human skin during its application so it is important that a clothing or blanket should be biocompatible with skin and also these should be biodegradable in context to their disposal [45]. Normally, the aerogel based fabrics (mostly nonwovens) are sandwiched between the two layers of different types of fabrics to avoid the direct contact of these fabrics with human skin. Therefore, alternative aerogels would be attractive for producing winter clothing and thermal blanket which do not have any harmful effects to the human skin.

Polysaccharides are organic biopolymers which are used to prepare aerogels from alginate, cellulose, pectin, starch, chitin and chitosan. These are biocompatible and biodegradable which make them attractive for various applications [18], [46], [47].

Additionally, alginate and cellulose aerogels are more flexible [48]–[52]. So, these may be good alternatives of silica aerogel for the formation of aerogel-nonwoven fibrous composites. The alginate and cellulose aerogels based nonwoven composites may serve as promising materials for thermal insulation, sound and liquid absorption and medical textiles.

Alginate is a sodium salt of alginic acid which is naturally occurring an organic material that is extracted from brown seaweeds. It is a linear copolymer of (1, 4)-linked β-D-mannuronic acid linked and α-L-guluronic acid. Alginate is a polysaccharide and was discovered by Standford more than a century ago which has been widely used in pharmaceuticals, food processing, textiles and paper formation for many years [53].

The alginate aerogels are prepared in four steps which involve: preparation of aqueous solution of sodium alginate, gelation of alginate, solvent exchange and drying.

To produce gel of alginate, an aqueous solution of required concentration is formed which depends upon the molecular weight of alginate. The aqueous sodium alginate has great affinity to make gel after reacting with aqueous solution of divalent cations. Therefore, the prepared alginate solution is combined with the solution with contains divalent cations such as Ca^{+2}, Ba^{+2}, Mg^{+2} and others. The divalent cations are believed to attach with carboxyl group from guluronic sites of alginate to cross-link the chains of polymer to form a gel network. After gelation, the gel is brought to solvent exchange to remove the water which is followed by supercritical drying in order to preserve the porous aerogel structure [54], [55].

Alginate aerogels have very low thermal conductivity and have great potential towards insulation applications. These aerogels have thermal conductivity as low as 0.018 W/mK, surface area as high as 680 m^2/g and porosity as high as 99.8 % [56], [57], [58].

Cellulose is another commonly used organic compound which is biodegradable and biocompatible biopolymer. Cellulose aerogels also have high surface areas (975 m^2/g), low densities (0.0005 g/cm^3) and high porosities (99.9 %). Cellulose aerogels are prepared by dissolving the cellulose or derivative of cellulose which is followed by the gelation of cellulose. Then, the solvent exchange or aging of cellulose gel is occurred. The solvent is removed from pore of cellulose by supercritical drying or freeze drying to get the solid porous structure of cellulose aerogel. The preparation of aerogel from cellulose carries some advantages over other aerogel precursors. These advantages are: cellulose as a raw material is renewable, no need of cross-linking agents for gelation and the chemical modification is easy as compared to other aerogel materials. The cellulose aerogels are used in thermal barriers, oil/water separation, source for carbon aerogels, metal oxide carriers and various biomedical applications [59], [60].

1.3 Aerogel-based Textile Composite for Wound Dressings

Though, the inorganic silica aerogels are used for some biomedical applications, but the organic aerogels like polysaccharides are proven to be more superior due to their nontoxicity, biocompatibility and biodegradability [18], [47], [61]. These aerogels are excellent materials for drug delivery, tissue engineering and wound dressings applications [62]–[64]. Wound care products demand has been increased across the globe.

Wound is a rupture or cut in skin resulting from any physical, chemical or thermal damage. These damages interrupt the functions of skin which are to protect the underlying tissues, bones and to regulate the body temperature. Therefore, it is essential to heal the wound as soon as possible to ensure the functioning of skin. Wound healing is a complex process which passes through four stages to achieve the complete growth and regeneration of tissues [65]–[67]. The first stage of healing process involves the prevention against microbial contamination and stoppage of blood loss. The second stage is a defensive or inflammatory which deal with formation of wound bed for the growth of new tissues. The filling of wound occurs in third step of wound healing which is called proliferative stage. The remodeling and maturation of wound come as a last stage which involves the formation of new tissues. This last wound healing step takes three weeks to two years depending on the category of the wound [68], [69].

The efficient and effective healing process can be attained through controlled environmental conditions at wound. These effective conditions can be achieved by controlling the microbes attack, provide vitamins and minerals and maintain moisture around wound. These conditions are successfully maintained by wound dressings in modern wound care management [70]–[72].

A wound dressing is a padding to dress the wound to promote the healing process. The dressing is different from gauze or bandages which are usually applied to cover the wound [73], [74]. The modern wound dressings have the ability to set moisture, provide antimicrobial resistance and can absorb the wound exudate. They are also loaded with several types of gels and drugs to protect and heal the wound. These modern wound dressing have been made from synthetic and natural materials and can be divide into several categories. These can be classified by their constituent materials and working mechanism such as hydrogel, hydrocolloids, collagen composites, alginates and tissue engineered skin substitute [75]–[77].

Hydrogel wound dressings are most suitable to maintain a moist condition at wound as these are composed of hydrophilic polymers. The chitosan and collagen polymers are usually used to structure hydrogel wound dressings in pad form which has outer nonwoven protection. The bovin-serum and glycosaminoglycan based hydrogel wound dressings are also produced [78]–[80]. Though, hydrogel dressings are nonirritant and elastic but have low mechanical strength and not showed desired results for heavy wound exudate [81], [82].

Hydrocolloid dressings carry two layers structure which interact with the wound exudate to form a gel on the wound surface. Usually, the outer protective layer is made from polyester nonwoven which hold the inner composite layer. The inner layer contains a gel forming component which can be a combination of gelatin, pectin or polyurethane. The Hydrocolloid dressings are not recommended for wounds with higher exudate [83], [84].

Collagen wound dressings are protein based bioactive dressings which form fibroblast on wound to accelerate the healing process by the migration of endothelial. These wound dressings are more effective for the wound with high exudate. The collagen layer contains various gels, polymers, alginates and cellulose derivative which able the dressing to absorb more wound exudate. Collagen wound dressings are also prepared in the form of pad by employing nonwoven fabric as a substrate [85]–[87].

The alginate based wound dressings promote the healing by keratinocytes migration on wound tissues [88]. It was also reported that alginate has the ability to accelerate wound healing by activating macrophages to develop TNF-α which initiates inflammatory signals [89]. The alginate is highly hydrophilic polymer that contains sodium and calcium salts having mannuronic and guluronic acid sites which forms gel when interacts with divalent cations like calcium. When alginate dressings interact with wound exudate, the layer of gel forms by ions exchange which helps to maintain the moisture environment at wound. The alginate dressings need a secondary dressing to avoid the dehydration of wound [84][90].

The tissue engineered skin substitutes which work like an artificial skin are employed for the wounds with extensive skin damage like burns. The skin substitutes consist of keratinocytes or dermal on collagen matrix along with fibroblast which stimulate the wound healing [91].

The commonly used wound dressings are mostly engineered in the form of composites which have an outer proactive layer to keep the inner wound interacting component. The outer layer of wound dressing is usually made from nonwoven fabric. Nonwovens are fibrous assemblies which are highly porous, light weight, low density and can easily be structured by using different raw materials. Therefore, nonwovens are considered suitable materials for wound dressings [80]. An ideal wound dressing has high porosity, moisture permeability, high surface area, flexibility and high mechanical strength [90][92][93].

Additionally, the wound dressing should also be bacterial resistant, biocompatible and nontoxic. In view of these requirements, the combination of an organic aerogel with nonwoven fabric may provide an efficient wound dressing.

1.4 Pure Aerogel Fibers as Alternative to Aerogel-based Textile Composites

The aerogel based textiles are normally produced by two techniques. The more commonly employed technique involves the formation of aerogel textile composites by the incorporation of fibrous assemblies into a solution which later is gelled, cured and dried. The fibrous assemblies which act as substrates can be woven, knitted and nonwoven fabrics. Glass wool, polyester and polypropylene fibers are commonly used to build these fabrics/laminates. In these aerogel textile composites, the aerogel component acts as resin while the textile fibers provide the reinforcement [94]–[97]

The second technique involves embedding the solid aerogel beads into the fibrous assemblies to build a nanoporous composite fabrics [7], [98]. The composites made by these two methods have low thermal conductivities, high sound and liquid absorption capacities. Aerogel blankets formed by incorporating silica aerogels into glass fibers have been commercially available for some time [99], [100].

Another strategy is to make aerogel based fabrics using pure aerogel fibers or fiber to fiber blend of aerogel fibers with conventional textile fibers. These fabrics may have interesting or superior properties. The syntheses of cellulose and silica aerogel fibers were reported recently in literature.

The cellulose aerogel fibers were formed by using a twin screw extrusion process by first dissolving cellulose in molten salt hydrate. Then, this solution was extruded to obtain gel fibers which were dried by using supercritical extraction to form cellulose aerogel fibers [101].

The silica aerogel fibers were produced by the sol-gel technique. Firstly, tetraethyl orthosilicate (TEOS), ethanol, water and a catalyst were mixed to get a homogenous solution. Then this solution was put into the fiber spinning assembly and extruded to form silica gel fibers. These gel fibers were supercritically dried to obtain silica aerogel fibers [102]. The silica and cellulose aerogel fibers were shown to have high porosities and low densities with properties comparable to the properties of the same type of aerogels in monolithic or bead form. Cellulose aerogel fibers also had good tensile strength and

flexibility [101]–[103].

As described earlier, alginate is an organic biopolymer which has some wonderful applications in biomedical, food processing, textiles and paper industries [104]. Alginate aerogels have very low thermal conductivity, low density, high surface area and high porosity [56]–[58].

Moreover, alginate aerogels have better mechanical properties and are categorized as viscoplastic materials. These aerogels can be bent like a paper up to 180°. The formation of alginate aerogels based PET composite for textile applications was recently reported in the literature. This alginate aerogel composite also had good mechanical and desirable pore properties. Therefore, alginate aerogels may have great potential for production of thermal clothing, liquid absorption fabrics, sound absorption fabrics and medical textiles [56], [105].

Alginate aerogel in the shape of fibers may have some additional flexibility which may be useful for preparation of aerogel based textiles for various applications. Actually, the fibrous forms of a number of materials like glass, ceramic and graphite were found to be more flexible and vibration resistant than their solid forms [102].

This work presents the formation of aerogel of aerogel textiles which were produced in forms of pure aerogel fibers and fibers reinforced aerogel composites. Two different kinds of composites were developed, one of these two was synthesized by the incorportion of alginate aerogel into PET nonwoven while the other was produced by the combination of cellulose aerogel with cotton nonwoven. Then, they were characterized by keeping in view of their area of applications. These aerogel based fibrous composites may be useful to produce fabrics for various appliations such as thermal insulation, sound absorption, liquid absorption and wound dressings.

Moreover, pure alginate fibers were synthesized from aqueous solution of sodium alginate by an extrusion process. These fibers are flexibile and carrying typical aerogels properties which can be employed to produce some novel textiles products.

Chapter 2

MATERIALS AND METHODS

2.1 Preparation of Alginate Aerogel PET Nonwoven Composite

To prepare alginate aerogel nonwoven composites, alginate source (Na-Alginate, Sigma Aldrich) was primarily dissolved in water to obtain 1.5 % by weight solution. A second aqueous solution was prepared with the gelation trigger, $CaCl_2$ (Sigma Aldrich) with a concentration of 0.2 M. Polyester Nonwoven fabric (PET nonwoven was taken from a blanket manufacturing company in Turkey) was firstly washed with pure ethanol and then dried in an oven to remove all possible impurities. The areal density of the PET nonwoven was in the range of 360 g/m^2.

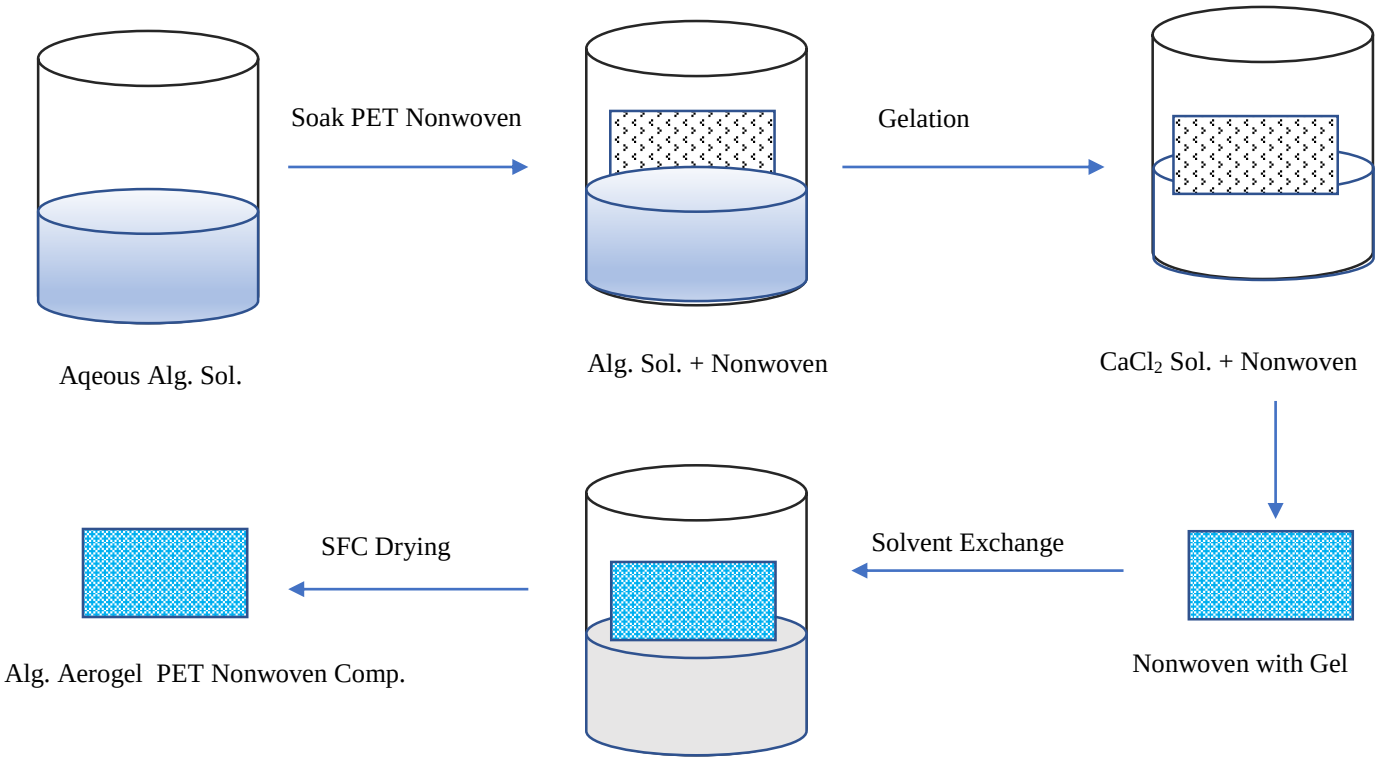

Figure 2.1: Schematic diagram of formation of alginate aerogel nonwoven PET composite

PET nonwoven was then placed in alginate solution and soaked overnight to allow the diffusion of the alginate inside the fabrics.The schematic diagram of process of formation of alginate aerogel PET nonwoven composite is shown in Figure 2.1.

Afterwards, it was taken out of the solution and immediately placed inside the $CaCl_2$ solution for gelation. The nonwoven fabric was left for 15 minutes in the $CaCl_2$ solution for ripening and then removed and washed with distilled water. The nonwoven was then successively subjected to a series of ethanol-water aging solutions of increasing ethanol concentration (10, 30, 50, 70, 90 and 100% ethanol) each with a duration of at least 30 minutes.

The last step was to dry wet composite gels at 90 bar and 313 K with supercritical carbon dioxide using an Applied Separations Speed SFE system with a 500 ml extraction vessel. Primarily, the vessel was filled with pure ethanol to prevent the contact of the composite samples with air and the synthesized composite was placed inside. Initially, ethanol which was used to fill the vessel was extracted. This was followed by extraction of ethanol from the pores of the samples to dry them completely, which took about 7 hours. Subsequently, the vessel was depressurized very slowly to prevent formation of cracks in the aerogel component. Beads of alginate aerogels were also produced separately using a similar procedure. The alginate solution was poured in to $CaCl_2$ with the help of burette to form beads. The ethanol-water aging and drying of these beads were done in similar way as were done for PET nonwoven composite.

2.2 Characterization of Alginate Aerogel-PET Nonwoven Composite

2.2.1 IR Spectroscopy

The synthesized alginate aerogel-fabric composite was characterized by Attenuated Total Reflectance (ATR) spectroscopy (Thermoscientific Nicolet IS10) to ensure the presence of alginate aerogel in the samples. The monolithic samples were cut in small dimensions before the measurements as required by sample size requirements of IR measurements.

2.2.2 XRD Analysis of Composite

X-rays diffraction (XRD), Bruker 08 Advance with CuKa radiation was used to determine the crystalline properties of pure PET nonwoven and alginate aerogel-PET nonwoven composite.

2.2.3 Thermal Stability Test of Composite

Thermogravimetric analyzer (TGA) Q500 was used to determine the thermal stability of pure alginate aerogel, pure PET nonwoven and of alginate aerogel-PET nonwoven composite. Samples were first dried and then were placed in aluminum pan which acted as a sample holder. The ramp rate was set at 5 ^{0}C/min and then all the samples were heated from 20 ^{0}C to 800 ^{0}C in nitrogen purge (60 mL/min).

2.2.4 SEM Analysis

To investigate the porous structures, SEM images were taken with Zeiss Ultra Plus Field Emission Scanning Electron Microscope after gold coating (4-5 nm).

2.2.5 Determination of Pore and Surface Properties of Composite

The average pore size, the pore volume and the specific surface area were determined by N_2 physisorption (Micromeritics ASAP 2020). The samples were primarily degassed at 353 K for 1 day prior to measurement to remove any impurities or solvent remaining in the pores. After determining the exact weights of the degassed samples, pore analysis was conducted using 60-point N_2 adsorption/desorption isotherms with a relative pressure (P/P_0) ranging from 10^{-7} to 1(which required at least 24 hours of continuous operation). The pore size distribution of the samples was determined using the Barret, Joyner and Halenda (BJH) method.

2.2.6 Thermal Testing of Composite by Alambeta Device

The thermal insulation, thermal diffusivity, thermal conductivity, and thickness of both pure PET nonwoven and alginate aerogel based nonwoven composite were measured using Alambeta device which employs a heat flow meter according to EN 31092 Standard as shown in Figure 2.2. Alambeta contains top and bottom plates between which the sample is inserted.Both plates have thermocouples and are set to different temperatures i.e. 40 ^{0}C for top plate and 32 ^{0}C for bottom plate.

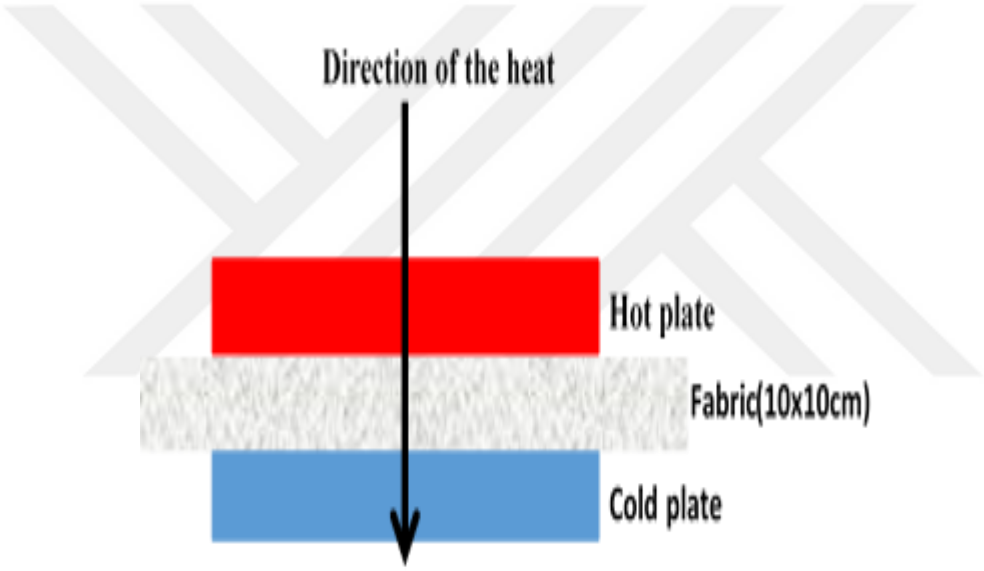

Figure 2.2: Principle of measurement of thermal properties of Pure PET nonwoven & alginate aerogel-PET nonwoven composite

After upper plate is lowered, the flow of heat is measured using a heat flow meter. The whole system is attached to computer programmed system. Alambeta has the capability of measuring both steady state and transient thermo-physical properties of compressible materials like textiles, biomaterials, foodstuff and liquids.

2.2.7 Thermal Imaging Test of Composite

Thermal imaging of pure PET nonwoven and alginate aerogel-PET nonwoven

composite was also conducted to estimate the thermal behavior qualitatively. FLIR seek thermal camera was used for thermal imaging. 5 cm x 5 cm specimens were cut from both fabrics and were placed on a hot plate. Temperature of the hot plate was maintained around 40 ^{0}C. It was made sure that the surface of the hot plate had even contact with both specimens to provide the uniform thermal radiation. The room temperature was kept around 20±2 ^{0}C. After both specimen were positioned on the hot plate, seek thermal camera was placed at a distance of around 40 cm from specimens. The images were captured after five seconds.

2.2.8 Tensile Strength Test of Composite

The stress-strain behavior of pure PET nonwoven and alginate aerogel-PET nonwoven composite was determined using a custom made tensile strength tester. Dog bone-shaped samples were cut according to ASTM D412-C standard which had width of 4mm and thickness of 4 mm. The samples were placed between the jaws of tensile tester with a gauge length of 35 mm and were stretched at a constant rate of elongation.

2.3 Preparation of Cellulose Aerogel Cotton Nonwoven Composite

The microcrystalline cellulose (MCC) was mixed with water and allowed it to swell at 5 ºC for 2 hours. Another solution was made by dissolving NaOH in water and cooled it to -6 ºC. Both solutions were prepared in such a proportion that in 100 g of solution, 7.6 g NaOH in 56.4 g of water and 6 g of cellulose in 30 g of water were added. These two solutions were mixed at -6 ºC and stirred at 1000 rpm for 2 hours. Then, a needle punched cotton nonwoven with areal density of 350 g/m^2 was immersed inside the prepared cellulose solution for 30 min to allow the diffusion of the cellulose inside the fabric. Afterwards, fabric was put inside the oven at 50 ºC for 2 hours where the gelation of cellulose occurred inside the nonwoven fabric. After gelation, the fabric was washed with distilled water and subjected to a series of acetone-water solutions of increasing acetone concentration (10, 30, 50, 70, 90 and 100 % acetone) each with a duration of at least 30 minutes. The process flow diagram of cellulose aerogel cotton nonwoven composite is shown in Figure 2.3.

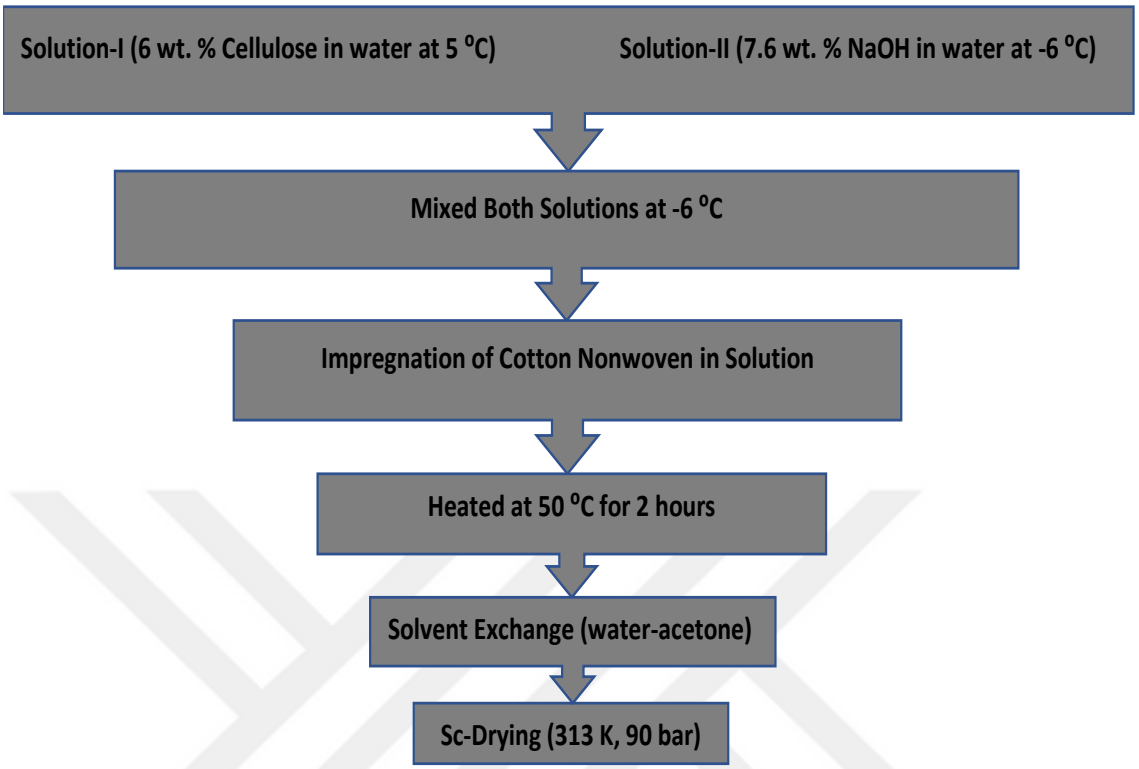

Figure 2.3: Process flow diagram of cellulose aerogel cotton nonwoven composite

The final stage was to dry wet cellulose gel inside the cotton nonwoven with supercritical carbon dioxide at 90 bar and 313 K using an Applied Separations Speed SFE system with a 100 ml extraction vessel. The vessel was filled with pure acetone and the synthesized composite was placed in it. Firstly, acetone inside the vessel was extracted which was followed by the removal of acetone from the pores of composite to dry it completely which took 6 to 7 hours to obtain cellulose aerogel cotton nonwoven composite. Subsequently, the vessel was depressurized very slowly to prevent formation of cracks in the cellulose aerogel. As cotton is a hydrophilic fiber so its was made sure that the composite was dried completely and no solvent left inside it.

The pure cellulose aerogel monoliths were also preapred. A mould was filled with cellulose solution and heated at 50 ºC where the gelation occurred after 2 hours. Then, solvent exchange and drying steps were performed as were done for cellulose aerogel nonwoven composite.

2.3.1 Loading of Silver Over Cellulose Aerogel Cotton Nonwovn Composite

To make cellulose aerogel cotton nonwoven resistant against bacteria, the loading of silver over the synthesized composite was done. The procedure for silver loading is similar till solvent exchange as is for the composite without silver. After solvent exchange, when the cellulose gel cotton composite is in 100 % acetone solution then 0.02 M solution of silver nitrate in acetone was prepared and the composite was soaked in it for 24 hours. The supercritical drying of this silver loaded composite was done in similar way as was done for the composite without silver. The process flow diagrame is shown in Figure 2.4.

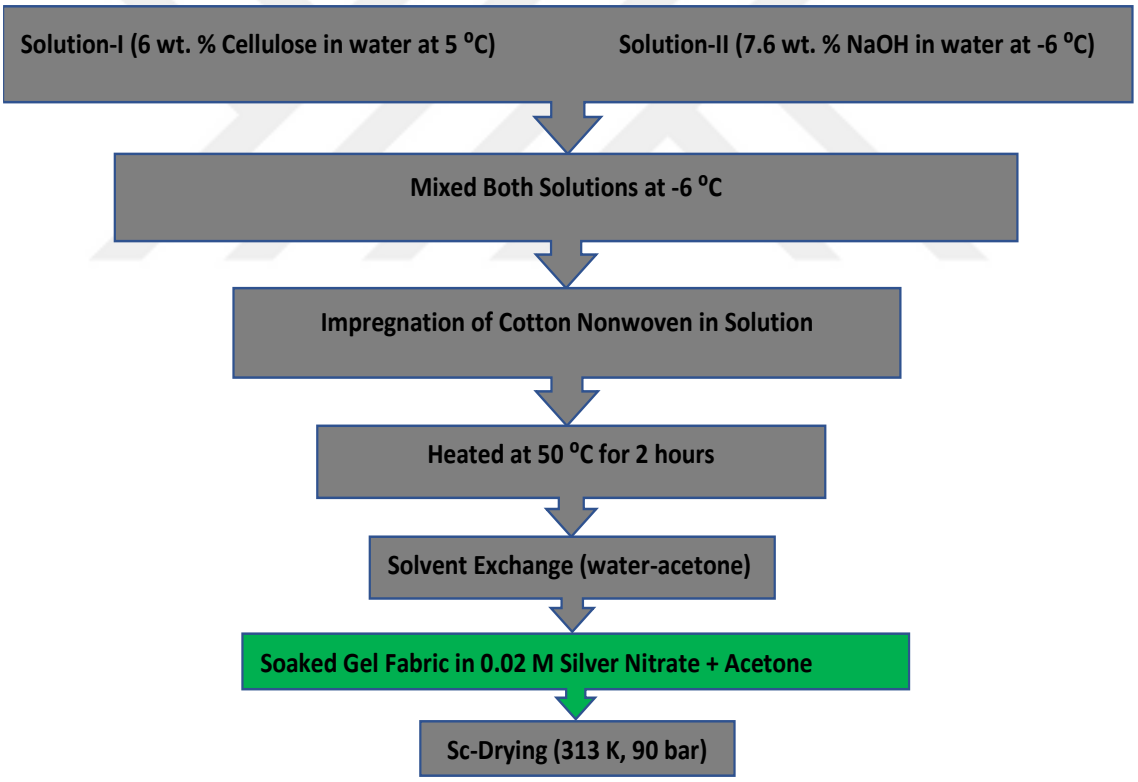

Figure 2.4: Process flow diagram of silver loaded cellulose aerogel cotton nonwoven composite

2.4 Characterization of Cellulose Aerogel Cotton Nonwoven Composite

The cellulose aerogel cotton nonwoven composite was characterized by Attenuated Total Reflectance (ATR) spectroscopy (Thermoscientific Nicolet IS10) to confirm the formation of cellulose aerogel inside the cotton nonwoven.

X-rays diffraction (Bruker 08 Advance with CuKa radiation) was used to observe the crystalline properties of pure cotton nonwoven and cellulose aerogel cotton nonwoven composite with and without silver.

The porous structures and morphology of cellulose aerogel cotton nonwoven composite were analyzed with SEM (Zeiss Ultra Plus Field Emission Scanning Electron Microscope).

The pore properties of composite were determined by N_2 physisorption (Micromeritics ASAP 2020). Firstly, the composite sample was degassed at 353 K for 24 hours before measurement for the removal of any impurities or acetone inside the pores. After determining the exact weights of the degassed samples, pore analysis was conducted using 60-point N_2 adsorption/desorption isotherms with a relative pressure (P/P_0) ranging from 10^{-7} to 1. Moreover, the pore size distribution of composite was determined using the Barret, Joyner and Halenda (BJH) method.

Differential Scanning Calorimetry (Netzsch STA 449 F3) was used to analyze the thermal stability of pure cellulose aerogel, pure cotton nonwoven and of cellulose aerogel cotton nonwoven composite. Samples were dried and put in aluminum pans which hold the samples. Then these samples were heated in nitrogen purge (20 mL/min) at ramp rate of 10 °C/min from 20 °C to 500 ^{0}C.

The core level binding energies of silver inside the cellulose aerogel cotton nonwoven composite were investigated by using X-ray photoelectron spectrometry (Thermo Scientific K-Alpha spectrometer).

2.4.1 Wound Exudate (Fluid) Absorbency Testing of Composite

The capacity of cellulose aerogel cotton nonwoven composite to absorb the wound exudate was tested by following the standard method of EN 13726-1:2002. Firstly, a solution was prepared by dissolving 2.298 g sodium chloride and 0.368 g calcium chloride dihydrate in 1 liter of water. This solution has same ionic composition as of wound exudate or human serum. The samples of 5 cm x 5cm were cut from pure cotton nonwoven and cellulose aerogel cotton nonwoven and their dry weights were measured.

The prepared solution was heated at 37 °C. Then, solution of weight equivalent to 40 time the weight of the each sample was taken and dispersed on them separately inside the Petri dishes. These samples were put inside the incubator at 37 °C for 30 min. After removal from incubator, each sample was picked from its respective Petri dish and hanged for 30 sec to remove excessive fluid.

The wet samples were weighted and fluid absorbency was recorded by following expression:

$$\text{Fluid Absorbency (\%)} = \frac{wet\ wt. - dry\ wt.}{dry\ wt.} X100$$

2.4.2 Antibacterial Activity Testing of Composite

The antibacterial activity of cellulose aerogel cotton nonwoven composite loaded with silver was determined by ATCC 25922 standard test method. The Escherichia coli strain was streaked on Mueller Hinton Agar (BD). Single colony inoculation was prepared in Cation Adjusted Mueller Hinton broth (BD BBL™ Dehydrated Culture Media) after overnight incubation. The inoculum was incubated at 37 °C with continuous shaking at 135 rpm for 8 hours. Then bacterial inoculum concentration was adjusted to 0.5 McFarland. The composite sample was sterilized by ultraviolet rays for 15 min before conducting the test. The prepared suspension was spread on Mueller Hinton Agar and sterilized sample was put onto the agar plate. This plate was incubated at 37 °C for overnight and inhibition zone was analyzed. For the control plate, whatman papers with 1 and 10 ug/ml ampicillin was prepared and zone inhibition was compared.

2.5 Synthesis of Flexible Alginate Aerogel Fibers

The low viscosity sodium alginate was purchased from Sigma Aldrich. Three different solutions with concentrations of 6 wt. %, 8 wt. % and 10 wt. % were prepared by dissolving sodium alginate in water. These solutions were stirred for 24 hours at room temperature. A 0.2 M aqueous solution of $CaCl_2$ was also prepared. Then alginate solution was filled into the syringe. A nozzle with a diameter of 800 µm was also attached to the tip of the syringe. Then the syringe was placed in a syringe pump. The alginate solution was then pumped into a $CaCl_2$ solution at a rate of 20 µL/min which led to the formation of alginate gel fibers in the $CaCl_2$ solution. The gel fibers were left for 15 to 20 minutes in the $CaCl_2$ solution for ripening. These fibers were then washed with water. The schematic diagram of extrusion of alginate aerogel fibers is shown Figure 2.5.

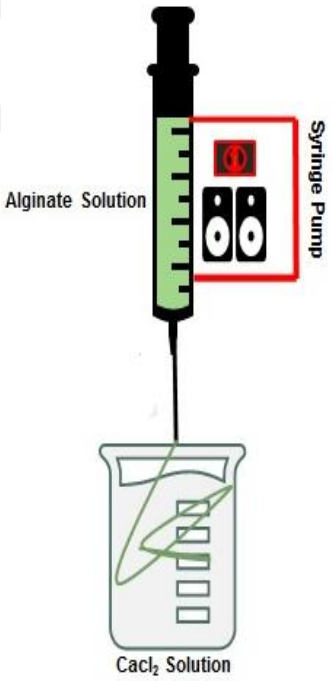

Figure 2.5: Schematic diagram of extrusion of alginate aerogel fibers

The solvent exchange and aging of these fibers was performed in ethanol-water solutions of increasing ethanol concentration (10, 30, 50, 70, 90 and 100% ethanol) each with a duration of at least 30 minutes. The alginate gel fibers are shown in Figure 2.6.

Figure 2.6: Alginate gel fibers

Finally, these alginate fibers at 90 bar and 313 K were dried using supercritical carbon dioxide to obtain aerogel fibers in an Applied Separations Speed SFE system. An extraction vessel with a volume of 100 ml was first filled with pure ethanol to avoid the contact of the alginate fibers with air. Then fibers were placed inside the ethanol filled vessel. The ethanol inside the vessel was extracted which was followed by extraction of ethanol from the pores of the fibers for 5 hours. The vessel was depressurized very slowly to prevent formation of cracks on alginate aerogel fibers.

2.6 Characterization of Alginate Aerogel Fibers

A stereo microscope (LEICA S9I) was used to take a series of images of gelation process of alginate fibers.

The pore structure of alginate aerogel fibers was observed by SEM (Zeiss Ultra Plus Field Emission Scanning Electron Microscope). The samples were coated with a 10 nm

thick gold layer. The images from the surface and cross-section of fibers were taken at different magnifications.

X-ray diffraction (XRD) was used to analyze the crystalline behavior of alginate aerogel fibers (Bruker 08 Advance with CuKa radiation).

2.6.1 Pore Properties of Alginate Aerogel Fibers by Mercury Porosimetery

The pore size, pore volume, surface area and bulk density of alginate aerogel fibers were determined by using mercury porosimetery (Micromeritics Autopore IV). The experiments were performed up to a pressure of 600 psia.

2.6.2 Alginate Aerogel Fibers Orientation Test by Raman Spectroscopy

The orientation of alginate aerogel fibers was determined with a Renishaw Invia-Raman microscope by using a 633 nm laser source. The light detector was placed parallel and perpendicular to the axis of fibers simultaneously to collect the scattered light.

2.6.3 Tensile Strength Testing of Aerogel Fibers

The mechanical properties of alginate aerogel fibers were determined using a tensile strength tester (Instron 4411) according to ASTM D3379-75. The tab for employing the fiber sample into the clamps of machine was prepared out of thick paper. A sample fiber was pasted at the ends of paper and the paper was cut from the center before mounting into the clamps. The purpose of this paper was to hold the sample into the clamps. The gauge length was fixed at 10 mm.

Initially a small pretension was given to fiber to remove any crimp or slackness and to rearrange the fibril to their original position. Then a tensile force at 2 mm/min was applied on the fiber sample till the complete deformation. The stress-strain graph of alginate aerogel fibers was plotted and elastic modulus was calculated at linear regions of the graph.

2.6.4 Thermal Stability Test of Alginate Aerogel Fibers

The thermal stability of aerogel fibers was determined by using Differential Scanning Calorimetry (Netzsch STA 449 F3). The samples were placed in titanium sample holder. Then aerogel fibers were heated from 25 °C to 650 °C at rate of 5 °C/min in nitrogen purge (20 mL/min).

Chapter 3

RESULTS AND DISCUSSIONS

3.1 Texture and Morphology of Alginate Aerogel-PET Nonwoven Composite

The alginate solution easily diffused into the PET nonwoven fabric because the nonwoven fabric had inherently high porosity. The shape and stability of the nonwoven fabric were preserved during the application of alginate solution. The gelation of this alginate solution was done by $CaCl_2$.

The images of alginate aerogel-PET nonwoven composite and pure PET nonwoven are shown in Figures 3.1 and 3.2 respectively. The surface and texture of alginate aerogel-PET nonwoven composite is neat and smooth. No dust was observed on the composite during its handling.

Figure 3.1: Alginate aerogel PET nonwoven composite

Figure 3.2: Pure PET nonwove

The IR spectra of PET nonwoven, alginate aerogel and aerogel-PET nonwoven composite are given in Figure 3.3. The peak at 1600 cm^{-1} confirmed the presence of sodium alginate in the nonwoven composite while the broad peak between 3000 cm^{-1} and 3500 cm^{-1} is due to the hydroxyl group of alginate. It was also observed that the spectrum of the composite had peaks from both the spectra of aerogel and PET.

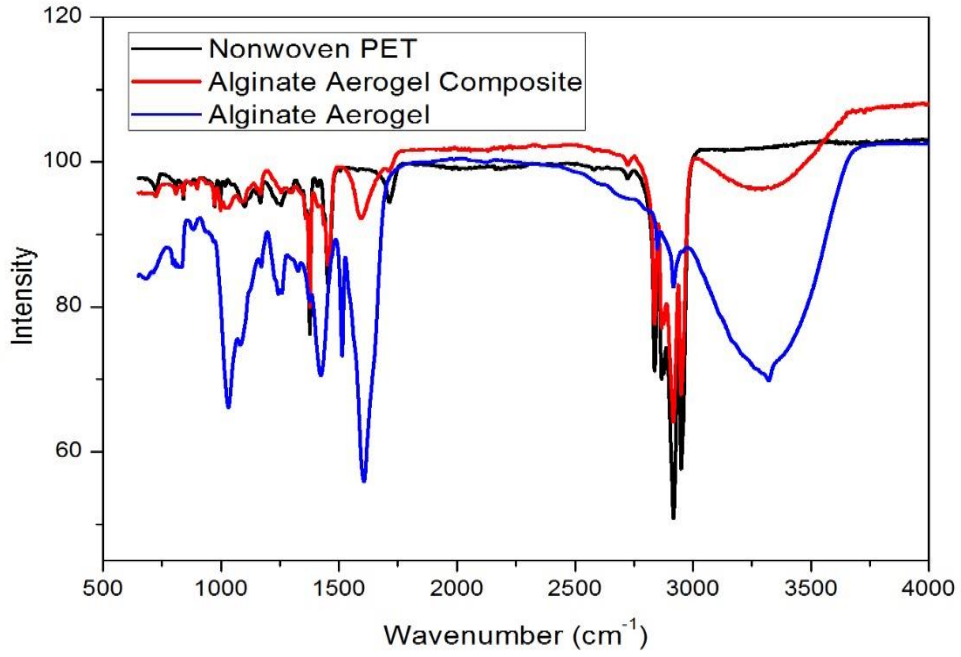

Figure 3.3: IR spectra of pure PET nonwoven, pure alginate aerogel & alginate aerogel-PET nonwoven composite

The X-ray diffraction patterns of pure PET nonwoven and alginate aerogel-PET nonwoven composite are presented in Figure 3.4. The characteristics peak at 22^0 is associated with alginate while the peaks at 18^0 and 27^0 are associated with PET. Alginate is an amorphous material while PET shows semi-crystalline properties which is also reflected by the XRD patterns of pure PET nonwoven and alginate aerogel-PET nonwoven composite. The associated peaks in alginate aerogel-PET nonwoven composite belong to PET and are not very sharp so that the composite has showed the semi-crystalline behavior.

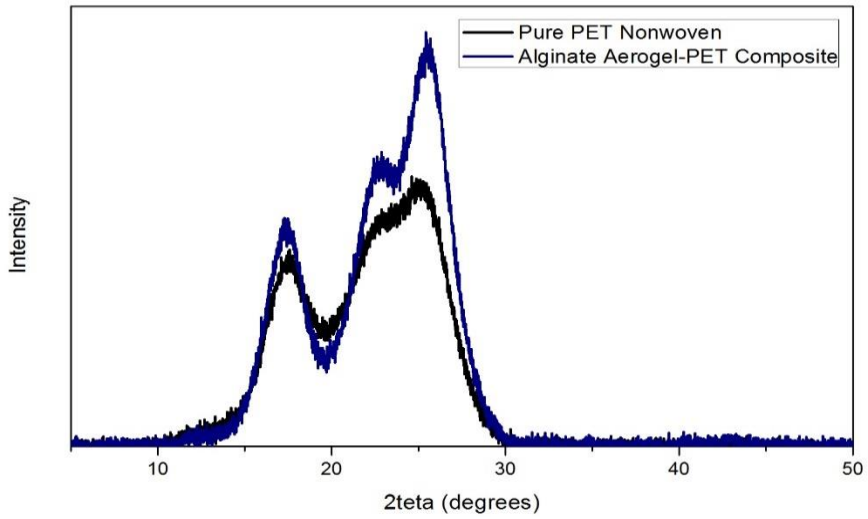

Figure 3.4: X-ray diffraction pattern of pure PET nonwoven and alginate aerogel-PET nonwoven composite

The N_2 adsorption-desorption isotherms of alginate aerogel based nonwoven composite at 77 K are shown in figure 3.5.a. It is clearly observed that the composite has type-IV adsorption isotherm according to IUPAC classification. The behavior of isotherm of alginate aerogel-PET nonwoven composite is truly in resemblance with isotherm of pure alginate aerogel as shown in Figure 3.5.b. Figure 3.6 shows the pore size distribution of the composite. Most of the pores are below size of 10 nm and are solely due to the result of the aerogel incorporation. The BET results are presented in Table 3.1 which show the significant difference between the properties of pure PET nonwoven fabric and alginate aerogel-PET nonwoven composite.

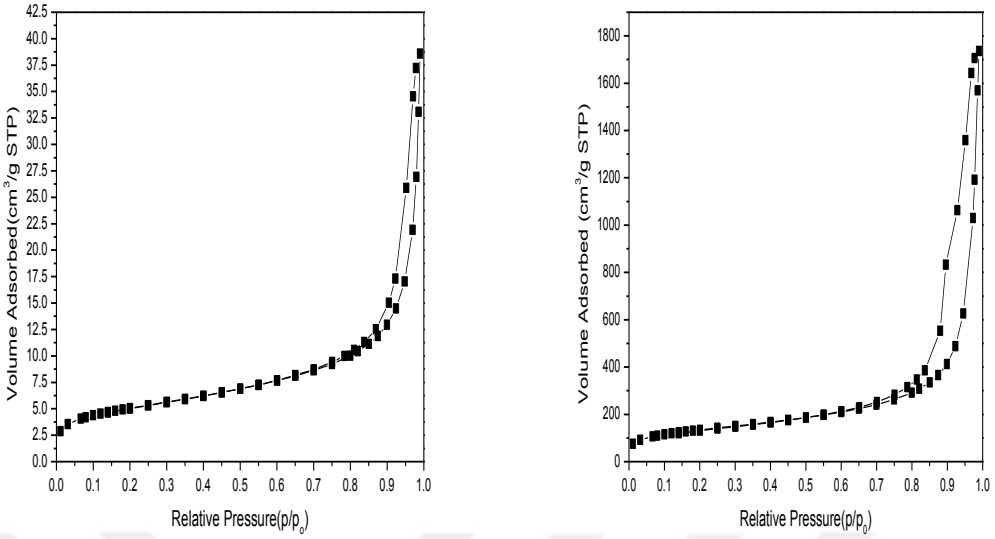

Figure 3.5: (a) N_2 ads. Isotherm of composite (b) N_2 ads. Isotherm of pure alginate aerogel

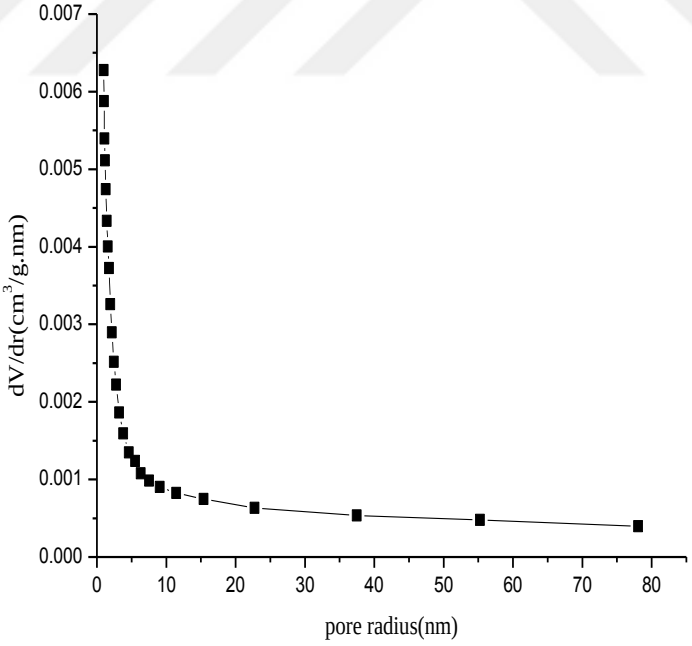

Figure 3.6: Pore size distribution of alginate aerogel in PET nonwoven composite

Table 3.1: Surface and Pore Properties by BET of alginate aerogel PET nonwoven composite

Sample Type	Surface Area (m^2/g)	Mean Pore Size (nm)	Mean Pore Volume (cm^3/g)
Alginate aerogel-PET nonwoven composite	18	7.9	0.06
Pure Alginate aerogels	345	6.2	0.66
Pure PET nonwoven	0.016	81.41	0.00058

Figures 3.7 (a-b) show the SEM images of pure PET and alginate aerogel-PET nonwoven composite. From Figure 3.7.a, one can see the pure PET network of fibers which are interconnected. Figure 3.7.b shows that the aerogel is incorporated in between and on the surfaces of these fibers. Figure 3.8 confirms that the alginate aerogel formed a porous structure in PET nonwoven.

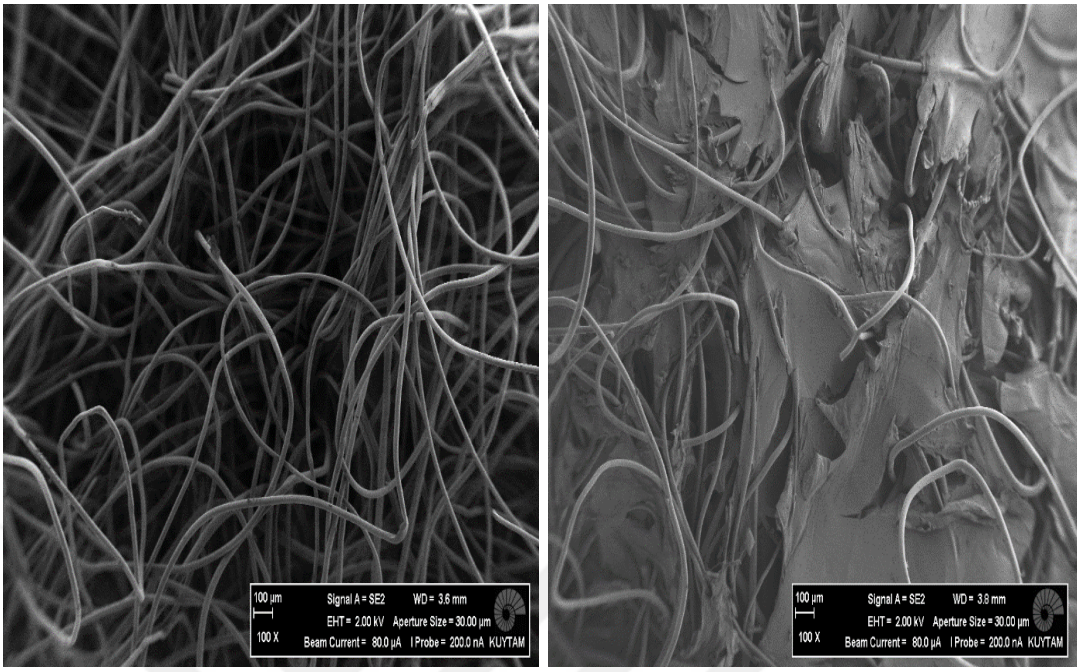

Figure 3.7: (a) PET nonwoven (b) Alginate aerogel-PET nonwoven composite

Figure 3.8: Porous structure of alginate aerogel inside the PET nonwoven composite

3.2 Thermal Properties Alginate Aerogel-PET Nonwoven Composite

Thermal resistance is an important parameter to characterize the thermal insulation properties of fabrics and is expressed by [106]:

$$r = \frac{h}{k} \quad \text{K m}^2\text{/W}$$

r = thermal resistance

h = thickness, m

k = thermal conductivity W/mK

The alginate aerogel-PET nonwoven composite has higher thermal resistance than pure PET nonwoven. Since alginate aerogel is a highly porous material and when it is incorporated into the PET nonwoven, the porous structure remains intact which is also confirmed by the SEM and BET analysis. The high porosity leads to a reduction in the thermal conductivity and increase in the thermal resistance. The thermal properties of pure PET nonwoven and alginate aerogel-PET nonwoven composite are given in Table 3.2. The thickness of the PET nonwoven increased after incorporation of the alginate aerogel into pure PET nonwoven resulting in an increase in the total volume. As the weight percent of alginate aerogel (having a very low density) within the composite is 17 %, the addition of the aerogel also increased the weight of the sample. The percentage increase in volume was more than the percentage increase of the weight resulting in a decrease of the overall density of the composite.

Generally, thermal conductivities of aerogel decrease with decreasing density due to the increase in pore volume and decrease in solid content. The nano-sized pores give rise to the Knudsen effect which results in the reduction of the thermal conductivity inside the pores to values less than air. Pure PET nonwoven structure is denser than aerogel and has more solid content in the form of fibers. Moreover, the pores are much larger. Therefore, the thermal conductivity for pure PET nonwoven is higher than aerogel.

The thermal conductivity of alginate aerogel-PET nonwoven composite is not significantly different than pure PET nonwoven. This may be due to small volume fraction of alginate aerogel present inside the fibrous structure of nonwoven which is only 17%.

Thermal diffusivity is another important parameter to describe the thermal behavior of aerogel based nonwoven composite. It describes the flow of heat through any medium (pure PET nonwoven or aerogel based composite in this case) and is calculated by the following expression:

$$a = \frac{k}{\rho.Cp} \quad m^2/s$$

k = thermal conductivity

ρ = density of fabric

C_p = Specific heat capacity of fabric

Thermal diffusivity of alginate aerogel-PET nonwoven composite is significantly lower than the thermal diffusivity of pure PET nonwoven. Alginate aerogel-PET nonwoven composite has a higher heat capacity (C_p) than pure PET nonwoven which is calculated by the above expression.

The alginate aerogel nonwoven composite is composed of PET fibers (solid), air and alginate aerogel. The alginate aerogel further consists of solid in its skeleton and air molecules present in its pores. The increase in heat capacity can be attributed to increasing solid amount in composite which is increased after loading alginate aerogel in PET nonwoven. Therefore, this increase in heat capacity has decreased the thermal diffusivity of alginate aerogel based nonwoven composite.

Table 3.2: Thermal properties of alginate aerogel PET nonwoven composite

Fabric type	Thickness mm	Thermal resistance mK m^2/W	Thermal conductivity W/m.K	Thermal diffusivity mm^2/s	Density kg/m^3	Heat capacity(C_p) J/Kg.K
Alg.aerogel-PET composite	4.34	110.6	0.0389	0.142	100	$2.7x10^3$
Pure PET nonwoven	3.4	83.4	0.0407	0.233	111	$1.6x10^3$

Thermal image of pure PET nonwoven and alginate aerogel based PET composite placed on a hot plate are shown in Figure 3.9. Positions of both fabrics are shown with their respective arrows i.e. alginate aerogel-PET nonwoven composite is on the right side and pure PET nonwoven is on the left side of the image. The color is different for both fabrics. It is clear from the thermal images that the alginate aerogel-PET nonwoven composite has hindered the flow of thermal radiation more than the pure PET nonwoven.

The blue color indicates a lower surface temperature than green. The reduced thermal flux to the surface for the alginate aerogel-PET nonwoven composite can be expected from its lower thermal diffusivity.

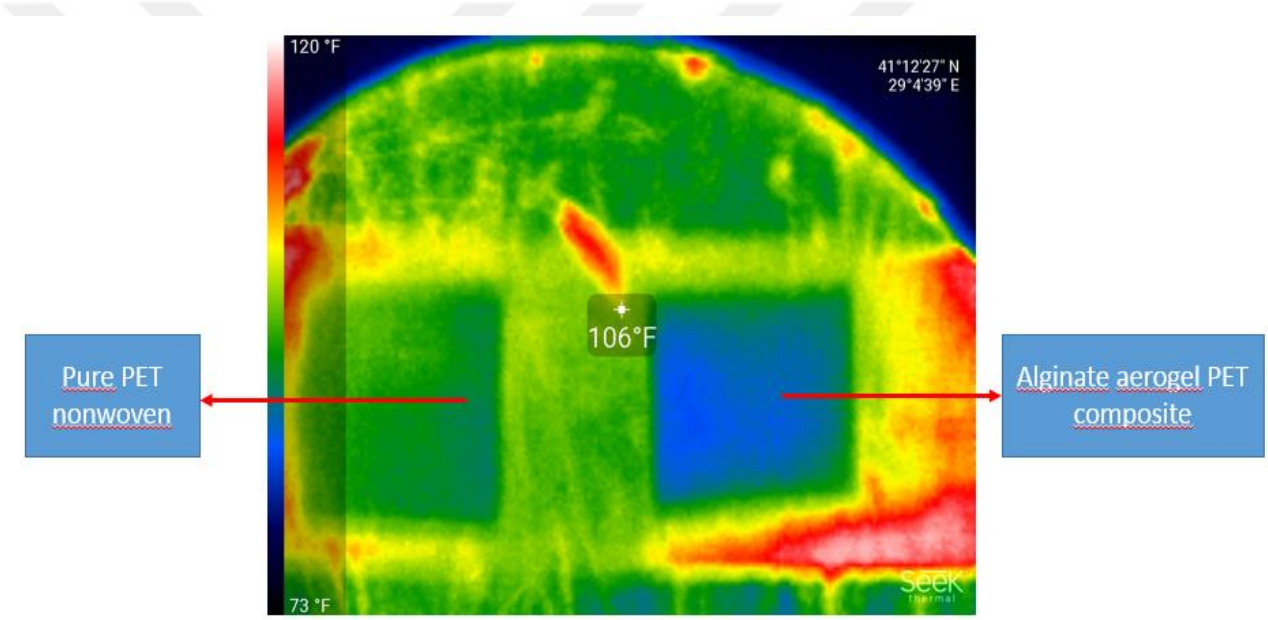

Figure 3.9: Thermal image of pure PET nonwoven VS Alginate aerogel-PET nonwoven composite

The TGA curves in Figure 3.10 have shown that the thermal degradation of alginate aerogel-PET nonwoven composite starts at 200 °C with a weight loss of 90 %. The weight loss from 0 °C to 100 °C is mostly likely due to moisture content while the weight loss from 200 °C to 300 °C can be attributed to alginate aerogel.

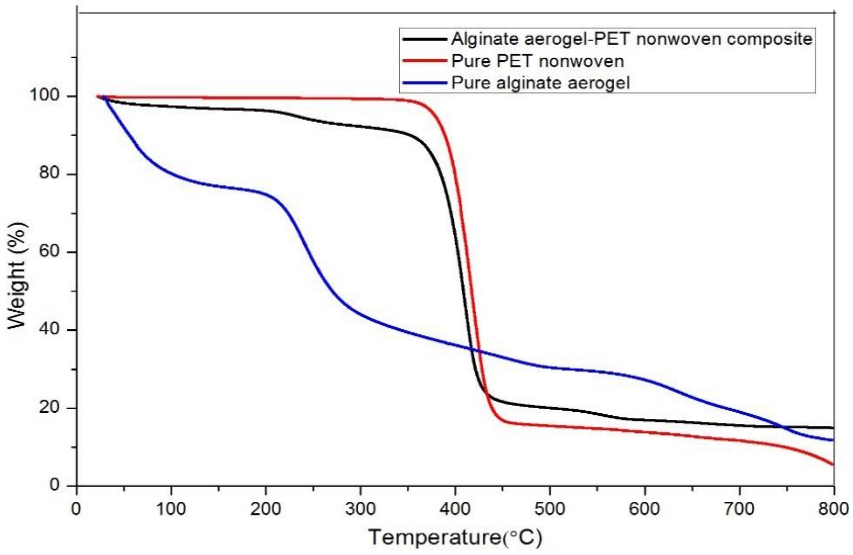

Figure 3.10: TGA curves of pure alginate aerogel, pure PET nonwoven and alginate aerogel-PET nonwoven composite

3.3 Mechanical Properties of Alginate Aerogel-PET Nonwoven Composite

The final strength of these types of composites is very important because in some cases the strength of composite may decrease due to various effects of different chemicals on the nonwoven fabrics. Figure 3.11 presents the stress-strain behavior of pure PET nonwoven and alginate aerogel-PET nonwoven composite. Stress-strain curves clearly show that the tensile strength of alginate aerogel-PET nonwoven composite is higher than pure PET nonwoven. The value of stress is higher for a specific amount of strain for composite than pure PET nonwoven. This increase may be due to the fact that the alginate aerogel forms layers between and on the PET nonwoven fibrous structure and acts as a resin to form the composite. Consequently, the bonding and interlinking of PET fibers has increased which caused the tensile strength of the composite to increase.

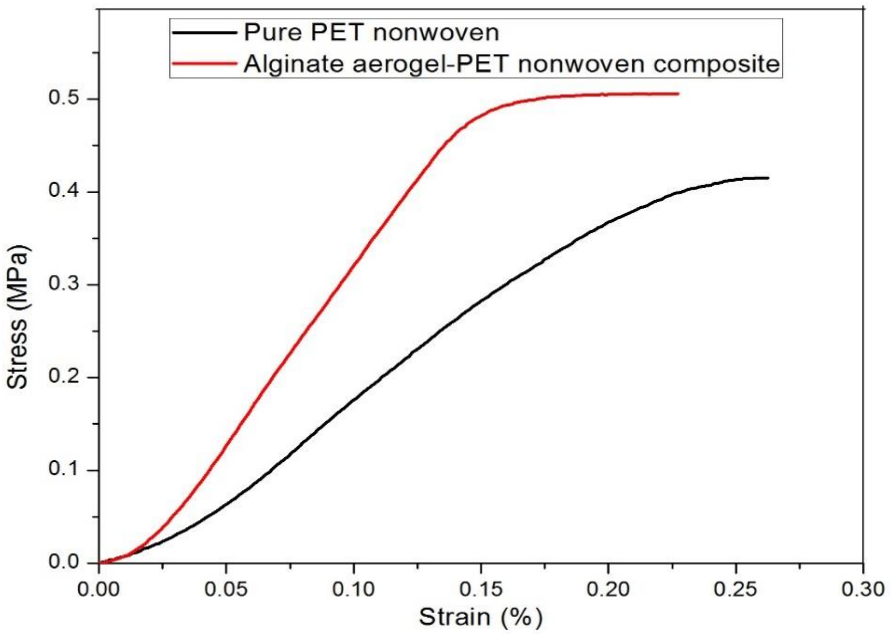

Figure 3.11: Stress-strain curves of pure PET nonwoven and alginate aerogel-PET nonwoven composite

3.4 IR Spectra of Cellulose Aerogel Cotton Nonwoven Composite

The IR spectra of pure cotton nonwoven, cellulose aerogel and cellulose aerogel cotton nonwoven composite are shown in Figure 3.12. The peaks around 1030 cm^{-1}, 1370 cm^{-1}, 1650 cm^{-1} 2900 cm^{-1}, 3300 cm^{-1} are attributed to C-O (stretching), C-H (bending), H-O-H, C-H (stretching) and O-H. The IR spectra of cellulose aerogel cotton nonwoven have peaks from pure cellulose aerogel and cotton nonwoven.

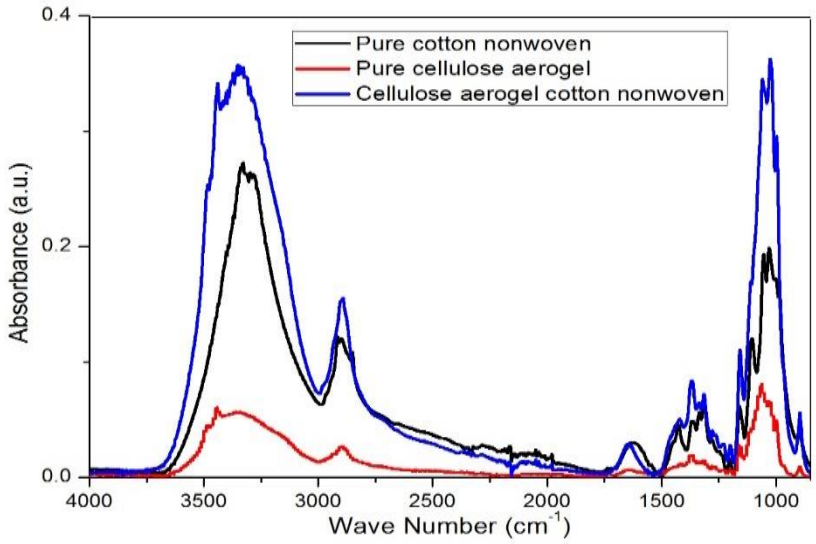

Figure 3.12: IR spectra of pure cotton nonwoven pure cellulose aerogel and cellulose aerogel nonwoven composite

3.5 Pore Properties of Cellulose Aerogel Cotton Nonwoven

The N_2 adsorption-desorption isotherms of cellulose aerogel cotton nonwoven composite at 77 K are presented in Figure 3.13. According to IUPAC nomenclature, the composite has shown similar behavior as of type-IV adsorption isotherm which means that the composite has mesoporous structure. Figure 3.14 shows the pore size distribution of the cellulose aerogel cotton nonwoven composite. The average pore size, pore volume and BET surface area of composite are 30 nm, 0.56 cm^3/g and 79 m^2/g respectively.

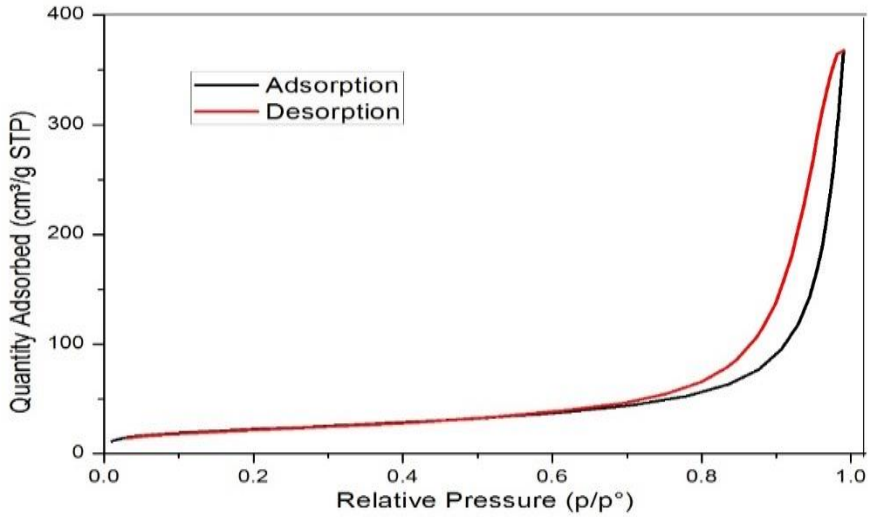

Figure 3.13: N_2 adsorption Isotherm of cellulose aerogel cotton nonwoven composite

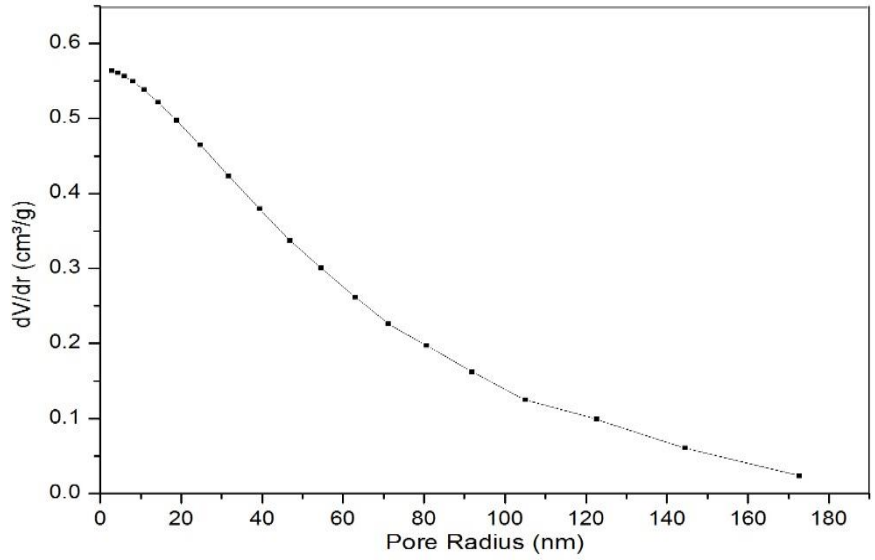

Figure 3.14: Pore size distribution of cellulose aerogel cotton nonwoven composite

3.6 Morphology of Cellulose Aerogel Cotton Nonwoven Composite

The Figures 3.15 (a-b) present the SEM images of pure cotton nonwoven and cellulose aerogel cotton nonwoven. The cotton fibers (Figure 3.15.a) are randomly oriented and have empty spaces inside the nonwoven fabric. After the incorporation of

cellulose aerogel, the blocks (Figure 3.15.b) of aerogel were formed between empty spaces of cotton nonwoven. The cotton retained its fibrous form after the incorporation of cellulose aerogel. The swelling of cotton fibers was observed (Figure 3.16) which may be caused due to the penetration of cellulose gel inside the amorphous regions of cotton fibers. The cotton fibers provided reinforcement while the cellulose aerogel acted as a resin to structure the composite. The porous structure of aerogel network inside cotton nonwoven can be seen in Figure 3.17.

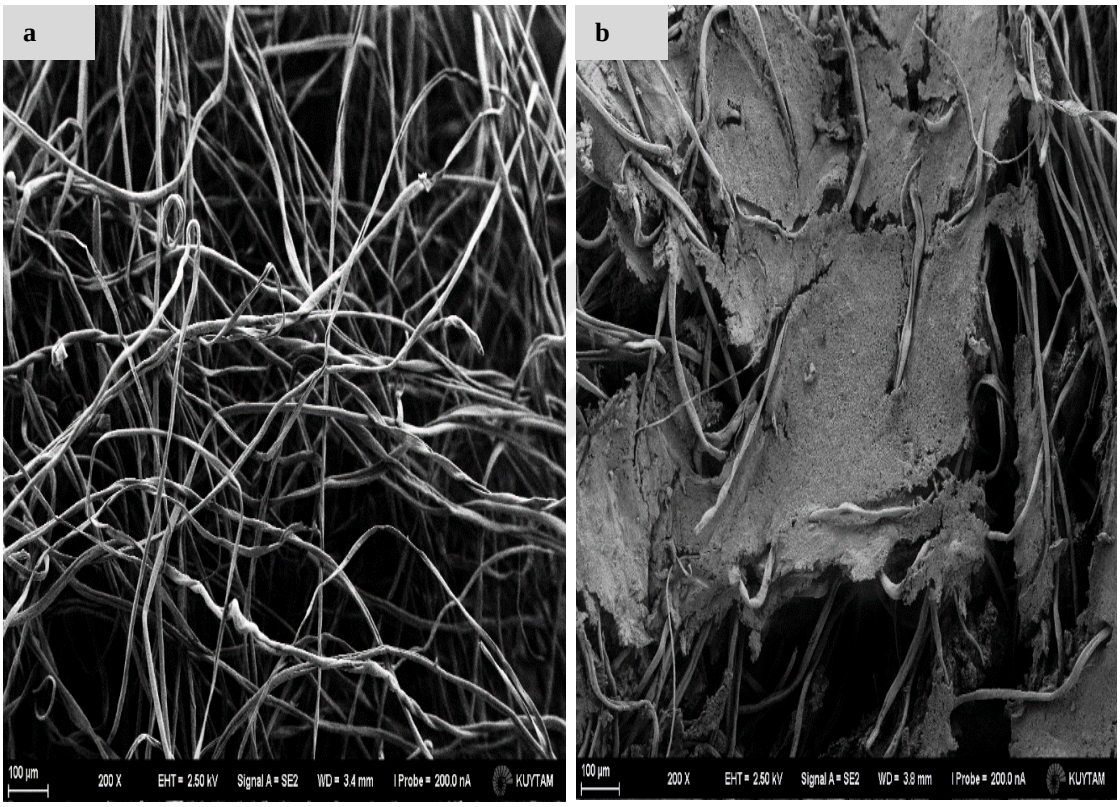

Figure 3.15: (a) Pure cotton nonwoven (b) Cellulose aerogel cotton nonwoven composite

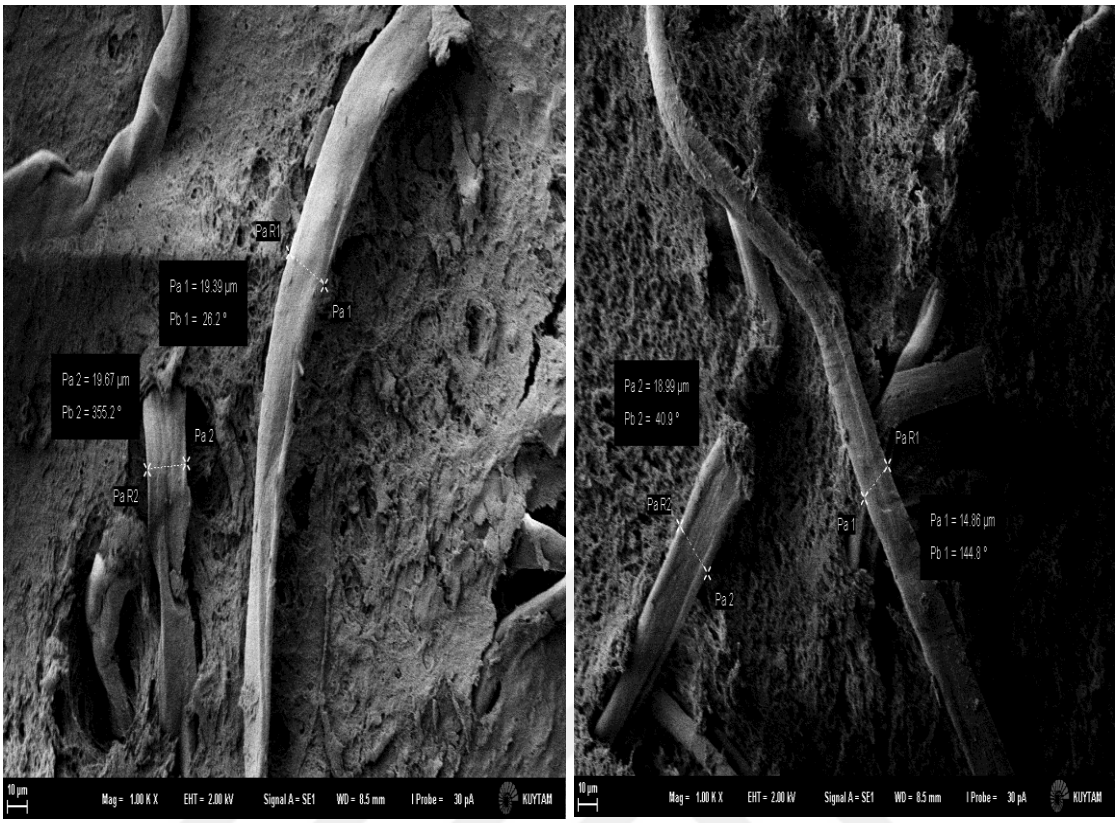

Figure 3.16: Cotton fibers inside cellulose aerogel

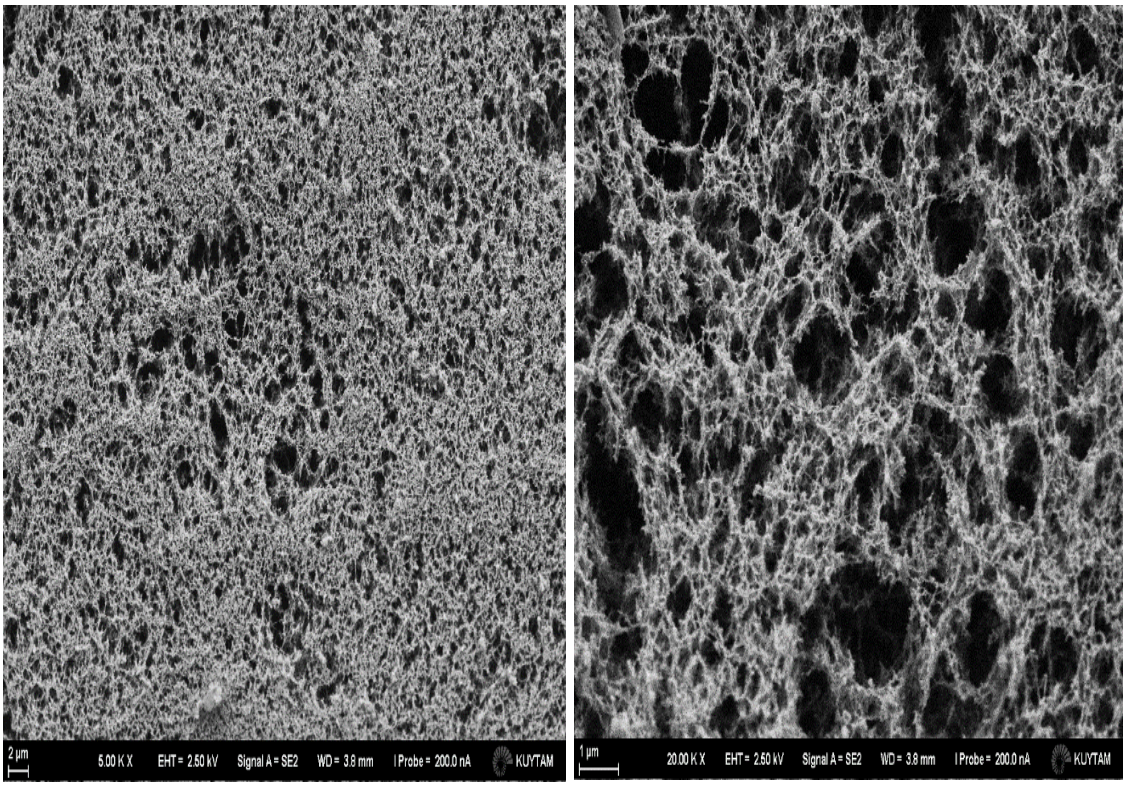

Figure 3.17: Porous structure of cellulose aerogel cotton nonwoven composite

The XRD spectra of pure cotton nonwoven and cellulose aerogel cotton nonwoven is shown in Figure 3.18. The peaks at 12° and 20° are belong to cellulose aerogel while the peaks at 14.7°, 22.4° and 33.9° are due to cotton fiber. Cellulose aerogel is an amorphous material while the cotton fiber has some crystalline regions which are reflected by the sharp peak at 22.4°.

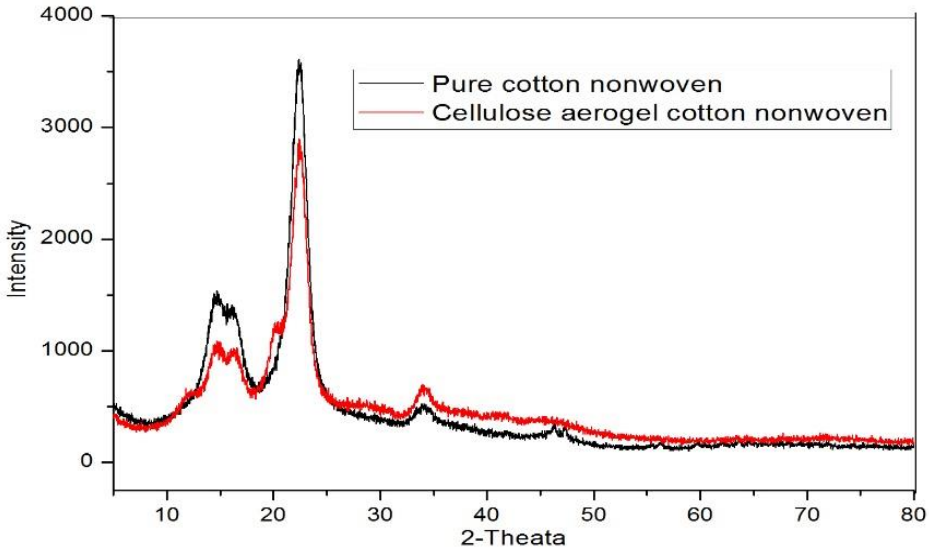

Figure 3.18: XRD spectra of pure cotton nonwoven and cellulose aerogel cotton nonwoven

The morphology of silver loaded cellulose aerogel cotton nonwoven composite is presented by SEM images in Figure 3.19 (a-d). The shiny silver can be observed (Figure 3.19.a) inside the cellulose aerogel cotton nonwoven which is uniformly (Figure 3.19.b) distributed in the form of silver nanoparticles with average diameter of 10 to 20 nm. The presence of silver nanoparticles was also confirmed by the sharp peaks in XRD spectra (Figure 3.20) of silver loaded cellulose aerogel cotton nonwoven composite. The sharp peaks at 43° and 54.4° represent the silver nanoparticles, these peaks are not present in XRD the spectra of cellulose aerogel cotton nonwoven composite.

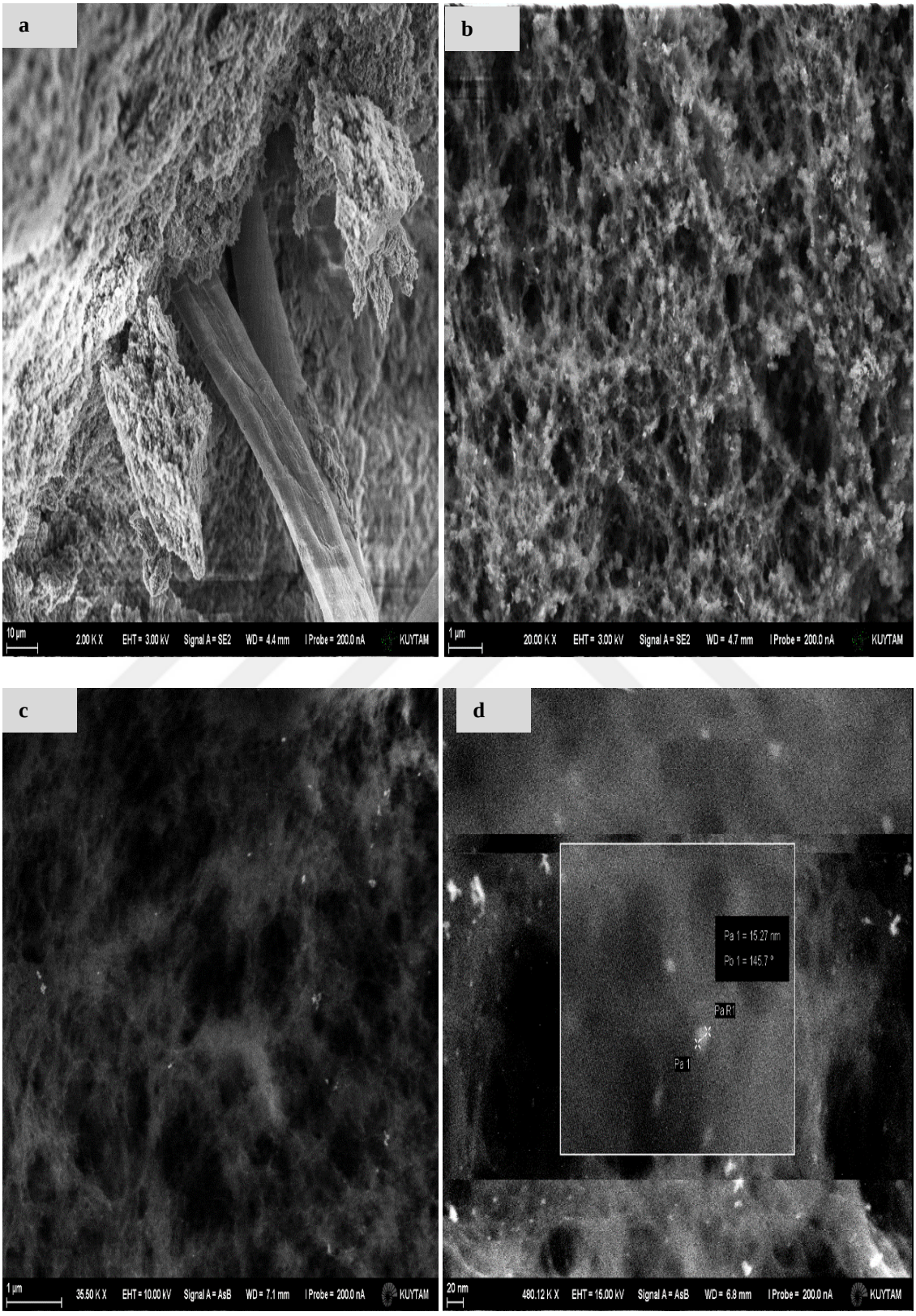

Figure 3.19 (a-d): SEM images of silver loaded cellulose aerogel cotton nonwoven composite

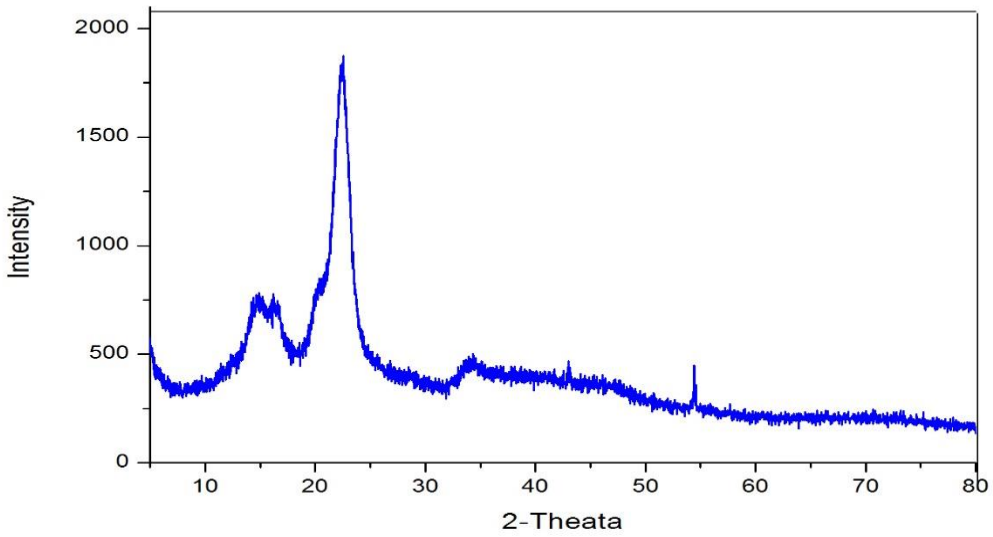

Figure 3.20: XRD spectra of silver loaded cellulose aerogel cotton nonwoven composite

3.7 Wound Exudate Absorbency of Cellulose Aerogel Cotton Nonwoven Composite

According to EN 13726-1:2002, the fluid absorbencies (wound exudate) of pure cotton nonwoven and cellulose aerogel cotton nonwoven were around 80 % and 300 % respectively. The nonwoven has highly porous structure whereas the cotton is a hydrophilic material. Therefore, the assembly of cotton in the form of nonwoven made it highly absorbent for fluid (wound exudate). Additionally, the aerogel is a superabsorbent material which is incorporated in the form of nanoporous blocks inside the cellulose aerogel cotton nonwoven. The images in Figure 3.21.b showed that the fluid droplet stayed on surface of cotton nonwoven but this was not the case for cellulose aerogel cotton nonwoven composite (3.21.a). The fluid absorbency of cellulose aerogel cotton nonwoven composite is three time the fluid absorbency of pure cotton nonwoven which is attributed to the porous structure of cellulose aerogel.

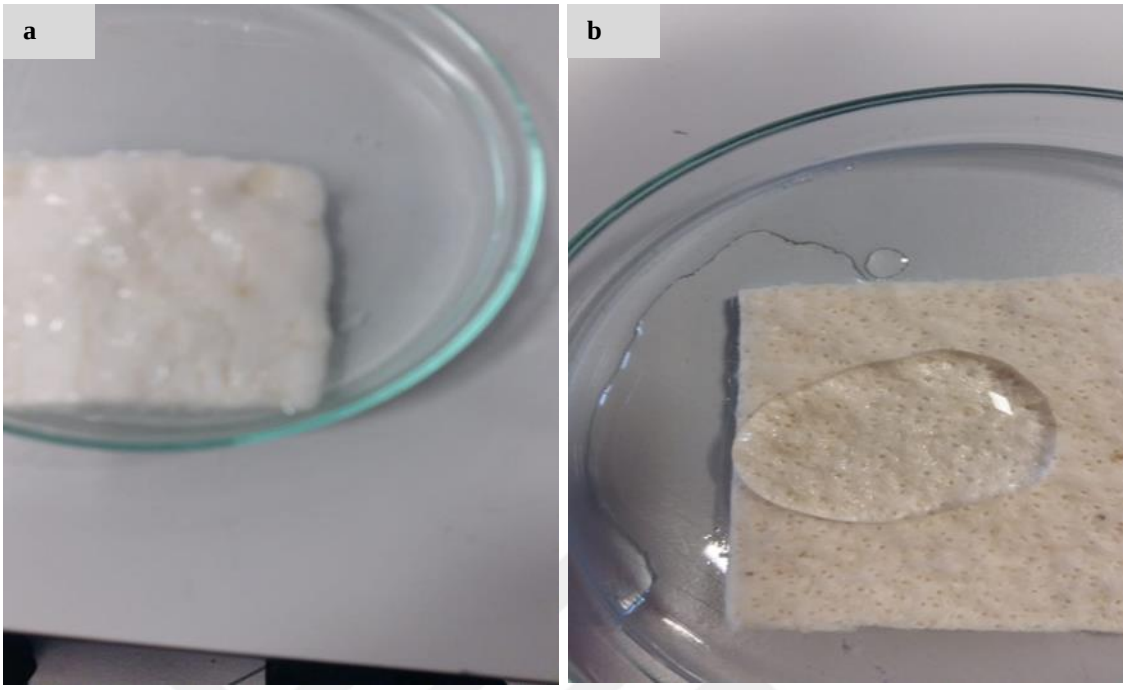

Figure 3.21: Wound exudate absorbency of (a) cellulose aerogel cotton nonwoven composite (b) pure cotton nonwoven

3.8 XPS Spectra of Silver loaded Cellulose Aerogel Cotton Nonwoven Composite

The XPS spectra of silver loaded cellulose aerogel cotton nonwoven composite is presented in Figure 3.22. The spectra showed the core level binding energies of Ag_5d_5 at 366.42 eV which is attributed to silver oxide (Ag_2O).

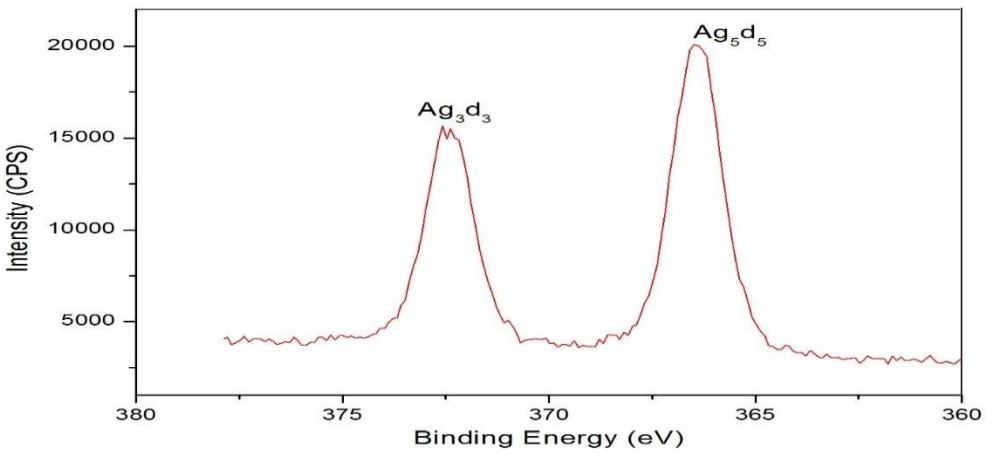

Figure 3.22: XPS spectra of silver loaded cellulose aerogel cotton nonwoven composite

3.9 Antibacterial Performance of Silver Loaded Cellulose Aerogel Cotton Nonwoven Composite

Figure 3.23 showed the photographs of antibacterial acivity against Escherichia coli by silver loaded cellulose aerogel cotton nonwoven composite and antibiotic control. The antibiotic control plates are shown to comapre it composite. A clear inhibation zone (marked with red arrows) was oberserved around the composite sample against the colonies of bacteria.

This inbibation zone was also formed around antibiotic control which can be compard with composite sample. As confirmed from XPS spectra that the silver was present in the form of its oxide (Ag_2O) which has the ability to kill the bacterias. The oxide form of silver is chemically active which damaged the RNA and DNA of bacteria and ultimatly caused its death.

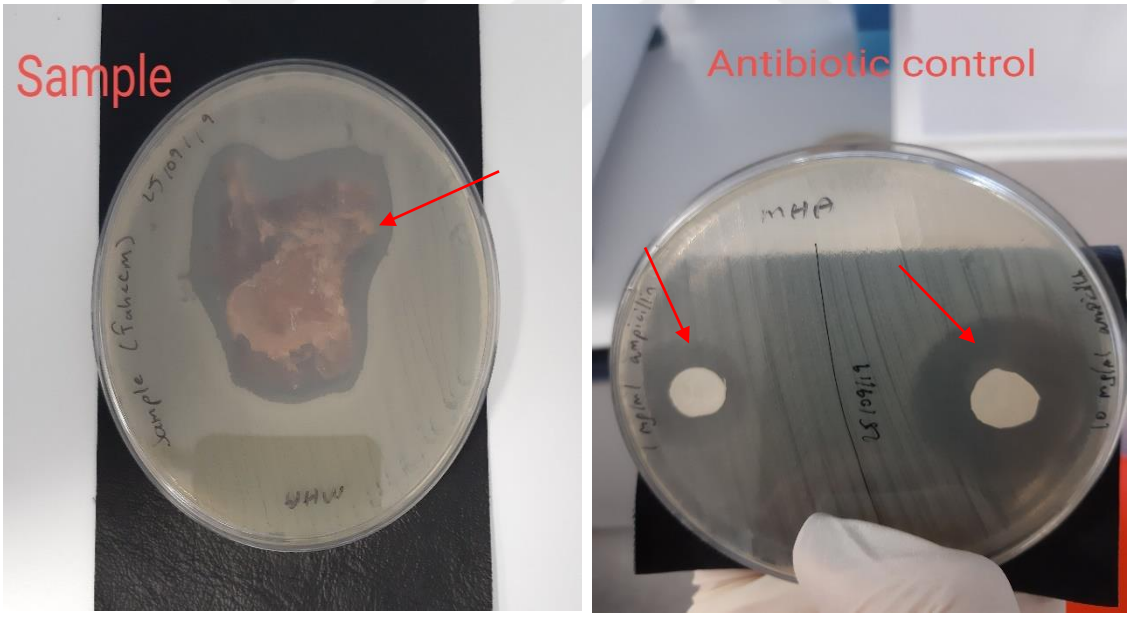

Figure 3.23: Photographs of antibacterial activity test of silver loaded compsoite sample and antibiotic control

3.10 Gelation Mechanism of Alginate Fibers

A minimum 6 wt. % of alginate solution was required to extrude the gel fibers in calcium chloride solution. It was observed that when the concentration of the alginate solution was below 6 wt. %, the gel did not keep the shape of fibers and formed a layer inside the calcium chloride solution. The similar finding was reported in literature that at least 5-6 wt. % of alginate solution is required for the preparation of alginate fibers. This was attributed to the direct relationship between viscosity of alginate solution and shaping (spinnability) it into the fibers, as at low concentration the required viscosity of fibrous dope cannot be reached [107].

A series of images with respect to time (2 minutes to 12 minutes) of the gelation of alginate fibers in calcium chloride solution by Stereo microscope are presented in Figure 3.24. The glass beaker contained aqueous solution of $CaCl_2$ was put under the microscope and fibers were extruded inside the beaker. The extrusion process was stopped after 2 minutes. As soon as the alginate solution was extruded from the syringe into the $CaCl_2$ solution, a thin calcium alginate layer formed on the surface of the sodium alginate stream. This resulted in preservation of the fibrous shape of the stream and prevented the mixing of the contents of the stream with the calcium chloride solution. The calcium alginate layer can be seen as a faint skin layer around the sodium alginate stream in Figure 3.24.a.

Initially, the fibrous gel and its center consisted of unreacted sodium alginate solution, but calcium ions diffused through this skin layer with time and reacted to form a complete calcium alginate gel fiber. The gelation of alginate was brought about by a cooperative binding of divalent calcium cations and the G-block regions of the polymer [108]. During this diffusion process, the boundary of calcium alginate gel layer moved toward the center of the fiber as shown in Figure 3.24 by the images of the fibers getting darker with increasing time from 4 minutes to 12 minutes. A decrease in the diameter of the gel fiber with time and thus a contraction in the volume of the gel was also observed as shown Figure 3.24. A similar shrinkage was also observed during gelation of alginate beads [109], [110].

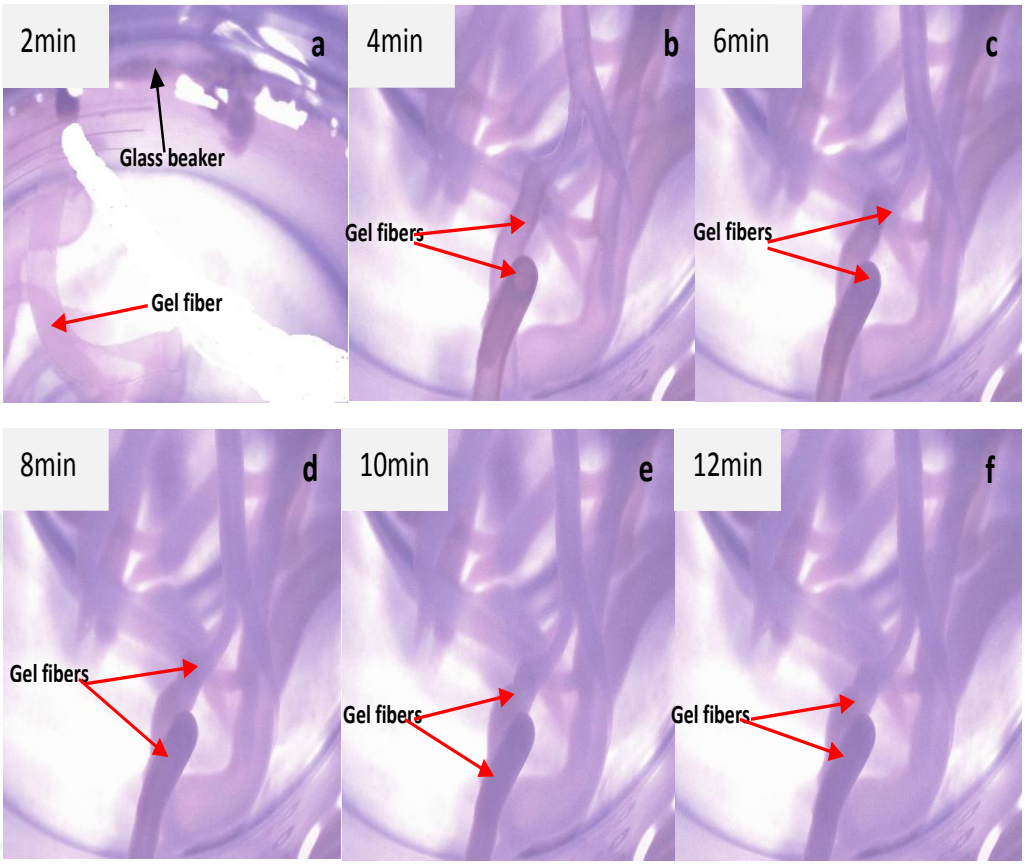

Figure 3.24. Series of images (6x) of gelation process of alginate fibers

The gel fibers were then dried using supercritical extraction and the aerogels fibers were obtained. Photographs of the alginate aerogel fibers are given in Figure 3.25. These aerogel fibers were easily bendable. They were in the forms of long filaments and staple fibers.

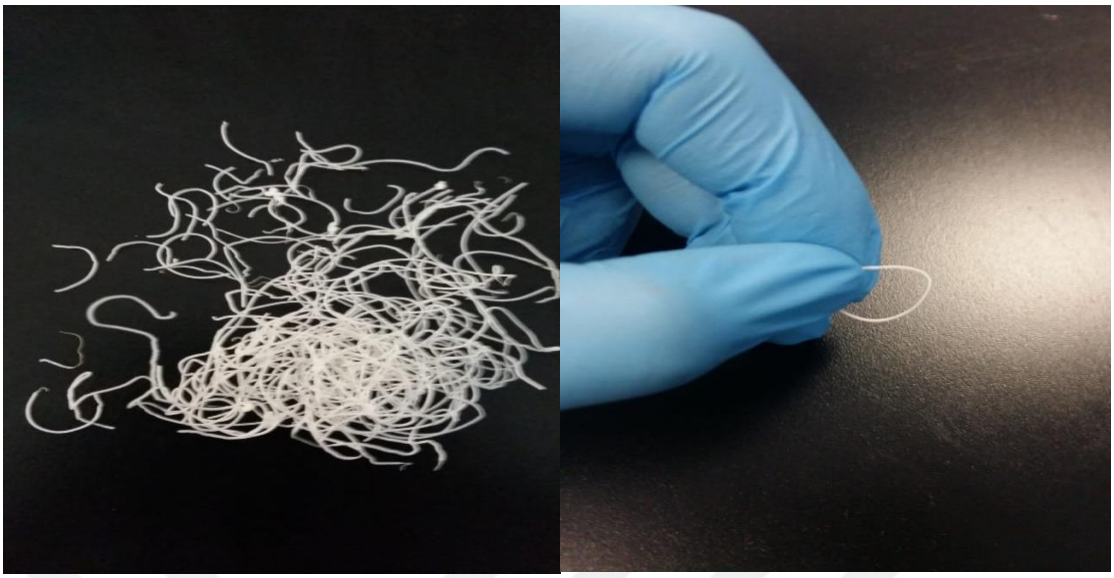

Figure 3.25: Dry alginate aerogel fibers

The diameters of the aerogel fibers are 410 μm, 470 μm and 530 μm for 6 wt. %, 8 wt. %, and 10 wt. % of alginate solution respectively as presented in Figure 3.26. The nozzle diameter was fixed at 800 μm for those three concentrations during the extrusion process. The increase in the fibers diameters by increasing the alginate concentration was observed. The cooperative binding of calcium ions with G-blocks sites of alginate was tighter in solution of low concentration of alginate as compared to high concentration. Therefore, the calcium-alginate polymer network in fiber became open in high concentration of alginate which increased the diameter of fiber [111].

3.11 Morphology of Alginate Aerogel Fibers

The aerogel fibers are cylindrical in shape and their surfaces display a smooth appearance. There are no visible pores on surface of fibers as can be seen in Figure 3.26.a.

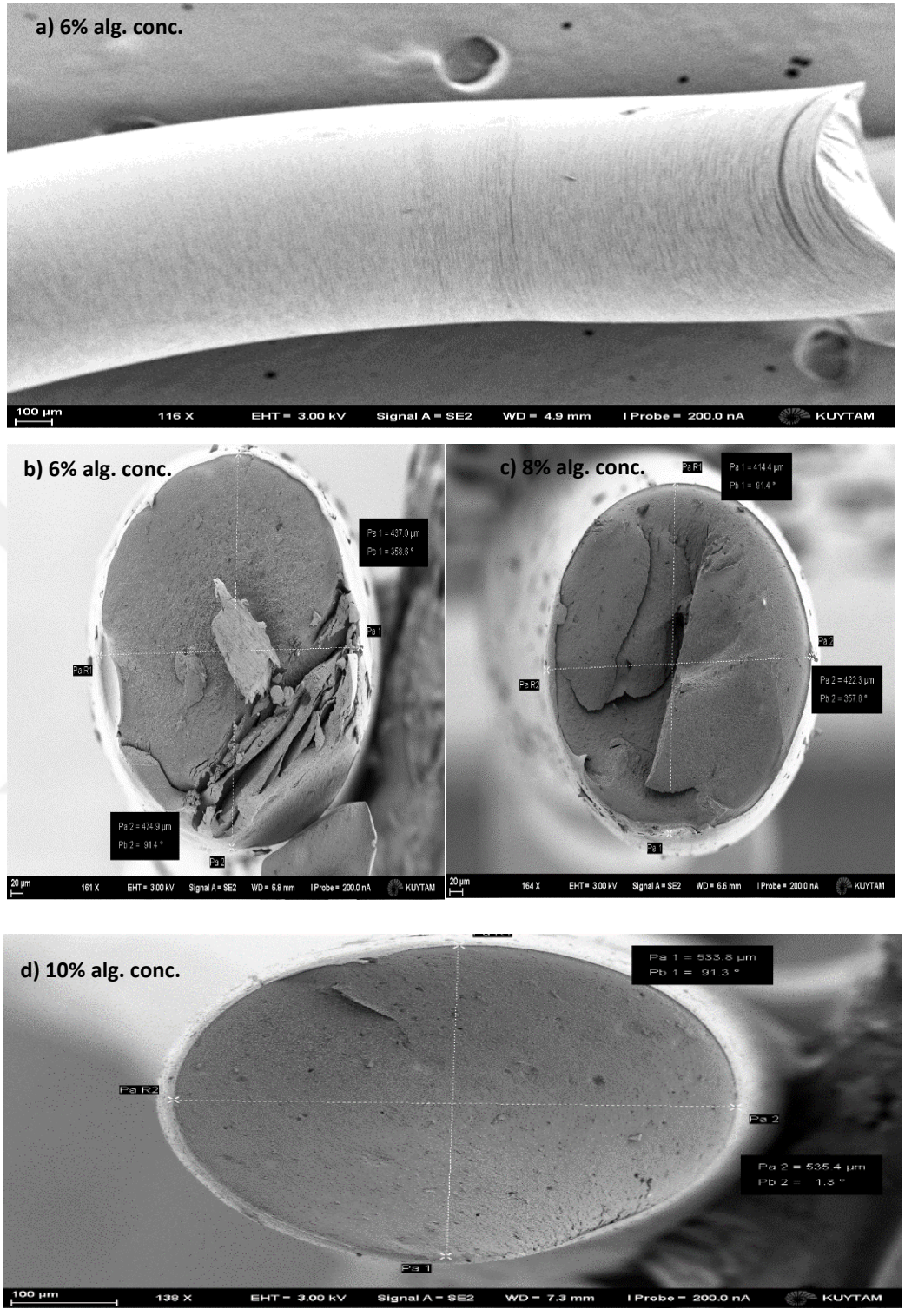

Figure 3.26: SEM images of (a) longitudinal & (b-d) cross-sectional view of single alginate aerogel fibers

The SEM images of single alginate aerogel fibers prepared using solutions with three different concentrations of alginate in water are given in Figure 3.27. Each single aerogel fiber contains number of microfibrils which are connected to form a web. The length of these fibrils is higher and more continuous for high concentration of alginate solution as can be seen in Figure 3.27. These SEM images also show that these aerogel fibers are highly porous. The pores are visible when fibers are cut from the cross-sections and aerogel fibers kept their original shape after cutting (Figure 3.26b-d).

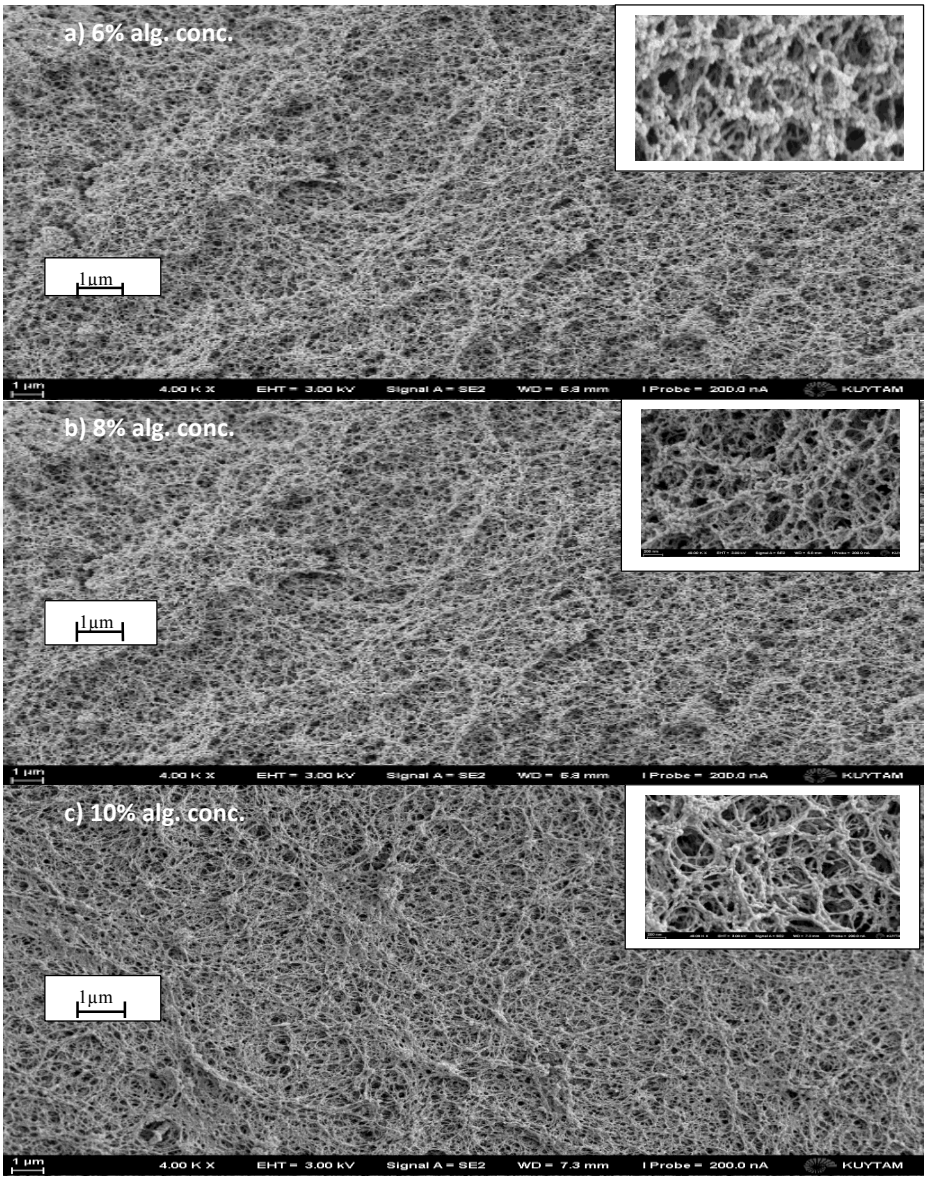

Figure 3.27: SEM images of alginate aerogel of single fiber (a) 6% (b)8% (c)10% concentrations of alginate in water

3.12 Pore Properties of Alginate Aerogel Fibers

The surface areas, bulk densities and porosities of alginate aerogel fibers were measured by mercury porosimetery which are given in Table 3.3. The average pore size ranged from 227 nm to 349 nm which is also in a good agreement with observed pore sizes from SEM images. The surface areas of alginate aerogel fibers (220 to 231 m^2/g) are high and are comparable to monoliths and beads alginate aerogels. The bulk densities (0.2 to 0.3 g/cm^3) are significantly higher than beads of alginate aerogels. The porosities of these fibers are also high but lower than monoliths and beads alginate aerogels which may be due to the higher weight percentages of alginate in water used in the extrusion process.

The alginate aerogel beads in the literature were synthesized by using 0.5 wt. % to 1 wt. % of alginate solutions whereas minimum 6 wt. % of alginate solution was used for these aerogel fibers. The pore properties of aerogel fibers do not depend on alginate content of the solutions used to prepare the fibers. It was also observed that the calculated bulk densities and the measured bulk densities were comparable.

Table 3.3: Surface and pore properties of alginate aerogel fibers by mercury porosimetery

Parameters	**6% Conc. of alginate**	**8% Conc. of alginate**	**10% Conc. of alginate**
Total Intrusion Volume (cm^3/g)	3.48	2.5	3.0
Surface Area (m^2/g)	225	220	231
Pore Diameter (nm)	349	227	247
Measured Bulk Density (g/cm^3)	0.24	0.32	0.27
Calculated Bulk Density (g/cm^3)	0.25	0.27	0.30
Porosity (%)	82.5	78	81.2

The X-ray diffraction patterns of alginate aerogel fibers are shown in Figure 3.28. There are no sharp peaks in the X-ray diffraction patterns which indicate that the alginate aerogel fibers are primarily amorphous. Small peaks were observed at 64° which show that there are some crystalline regions in the fibrous structure. During extrusion, the gel was formed in longitudinal direction which may have created the ordered domains in the form of small fibrils inside the fiber.

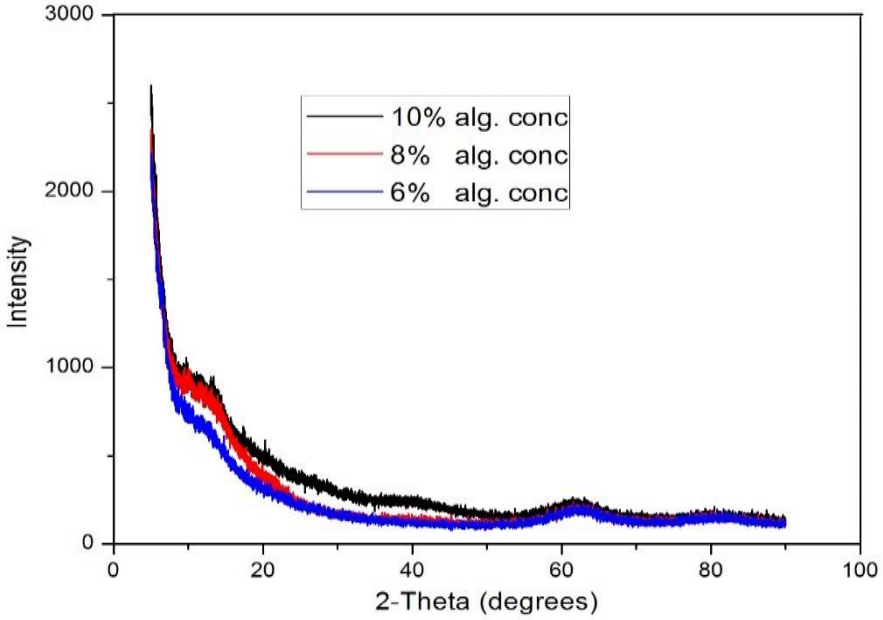

Figure 3.28: X-ray diffraction patterns of alginate aerogel fibers

3.13 Mechanical Properties of Alginate Aerogel Fibers

The stress-strain behavior of alginate aerogel fibers are presented in Figure 3.29 which showed that both linear and non-linear elastic regions exist for fibers prepared with 6 wt. % and 8 wt. % of alginate solutions. The stress-strain curve for these types of fibers is non-linear till 9 % of strain but afterwards the curve is quite linear. The aerogel fiber prepared using 6 wt. % of alginate solution showed higher stress values than fiber prepared with 8 wt. % of alginate solution till 9 % of strain. The fibrils inside the aerogel fiber prepared using 6 wt. % of alginate solution could not withstand the high tensile stress after 9 % of strain and their tensile stress kept on decreasing until fiber deformation occurred at stain of 15 %.

The aerogel fiber prepared using 8 wt. % of alginate solution showed some deformation at a strain of 13 % but it did not fracture completely. It seemed that few fibrils inside the fiber were broken and then others repositioned themselves against the tensile stress at strain of 13 %. The complete deformation took place at 14 % of strain for aerogel fiber prepared using 8 wt. % of alginate solution. The stress-strain behavior is quite linear till the fracture point for the fiber prepared with 10 wt. % of alginate solution. The alginate aerogel fibers have elastic moduli (at a strain of 10 %) of 0.25 MPa, 0.29 MPa and 0.45 MPa for 6 wt. %, 8 wt. %, and 10 wt. % of alginate concentrations in water respectively.

The results of single fiber tensile test showed that the tensile strength and tensile strain depend upon the concentrations of alginate in water for these aerogel fibers. Their maximum tensile stress increased whereas the maximum tensile strain has decreased with increase in concentrations of alginate in water.

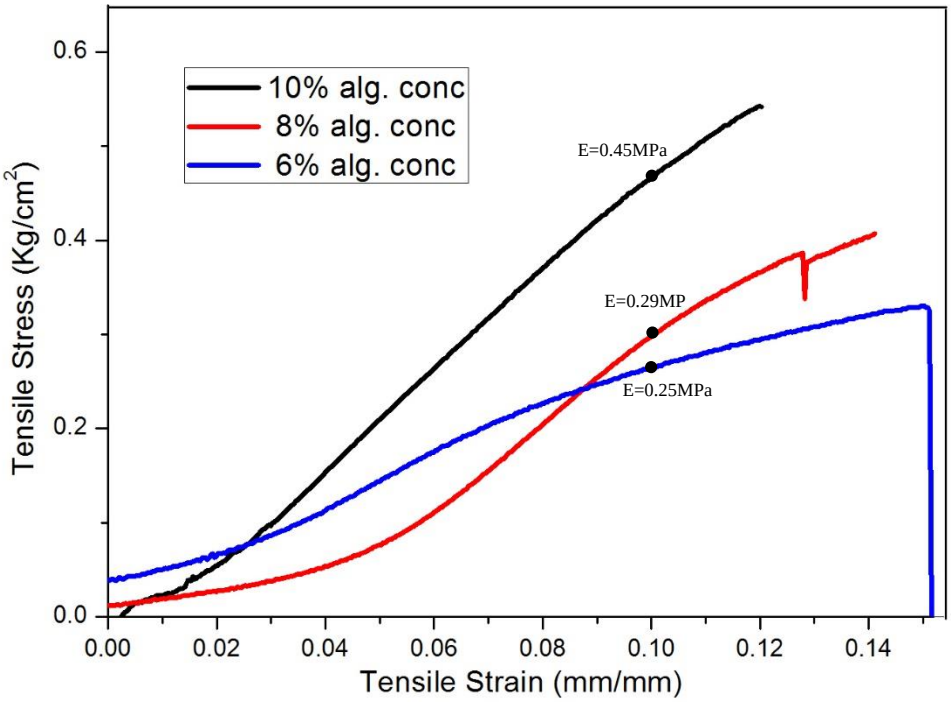

Figure 3.29: Stress-strain diagram of alginate aerogel fibers

As more solid in the form of fibrils is present in aerogel fibers prepared using higher concentrations of alginate solutions, which caused the stronger aerogel fibers. Moreover, as number of fibrils per cross section of fiber is higher so these have less space among them. Therefore, the fibers prepared using higher wt. % of alginate solutions have low flexibility.

The strength of alginate aerogel fibers also depends on the length of fibrils inside the aerogel fibers. These fibrils are longer for fibers prepared using 10 wt. % of alginate solution (Figure 3.27) which made them stronger as compared to the fibers prepared using 6 wt. % and 8 wt. % of alginate solutions.

The orientation/arrangement of fibrils inside the fibers is an important factor which controls mechanical properties [8]. The fibers have high strength and low flexibility if the fibrils are uniformly oriented in the direction parallel to fibers axis. The orientation of aerogel fibers was observed by Raman spectroscopy. Raman spectra of aerogel fibers formed by using 6 wt. %, 8 wt. %, and 10 wt.% concentrations of alginate in water are shown in Figure 3.30 (a-c). The depolarization ratio (D.P) can be used for the determination of fibers orientation. So, the depolarization ratio was calculated by dividing the intensity of scattered light from perpendicular to fiber axis with parallel to fiber axis for symmetric carboxylate stretching vibrations at 1300 cm^{-1} and 1413 cm^{-1}.

The D.P ratios (Table 3.4) of aerogel fibers prepared using 10 wt. % of alginate concentration is lower as compared to 6 wt. % and 8 wt. % for both peaks. It shows that the fibers prepared using 10 wt. % alginate solution are more anisotropic and fibrils are oriented in the direction of fiber axis rather than in other directions. Because the fibrils are more oriented in the direction of fibers, these fibers have higher tensile strength and lower tensile strain.

Similarly, the fibers prepared using 8 wt. % of alginate solution are more oriented in direction of their axis as compared to fibers with 6 wt.%. So, they are stronger and less flexible. These observations are also in an agreement with the results of tensile strength test. The extrusion of fibers occurred in the direction of fiber axis, so all the fibrils supposed to be oriented in the fiber axis. But the fibers do not have fully anisotropic structure.

Table 3.4: Depolarization ratios for alginate aerogel fibers

Raman shift (cm^{-1})	Wt.% of alginate in water	D.P ratio
1300	6	0.6
1300	8	0.4
1300	10	0.37
1413	6	0.2
1413	8	0.2
1413	10	0.17

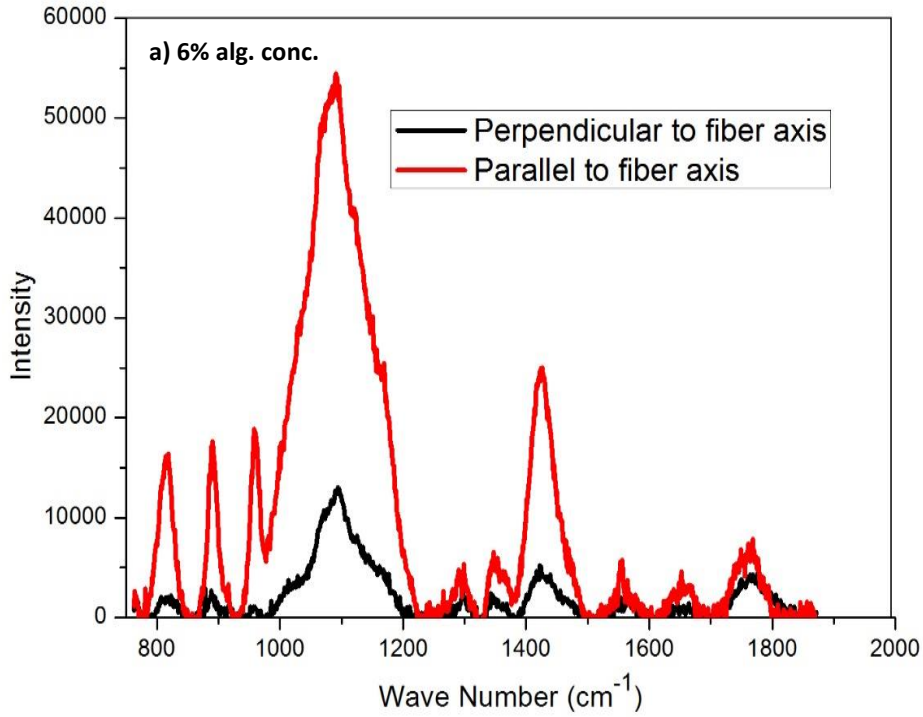

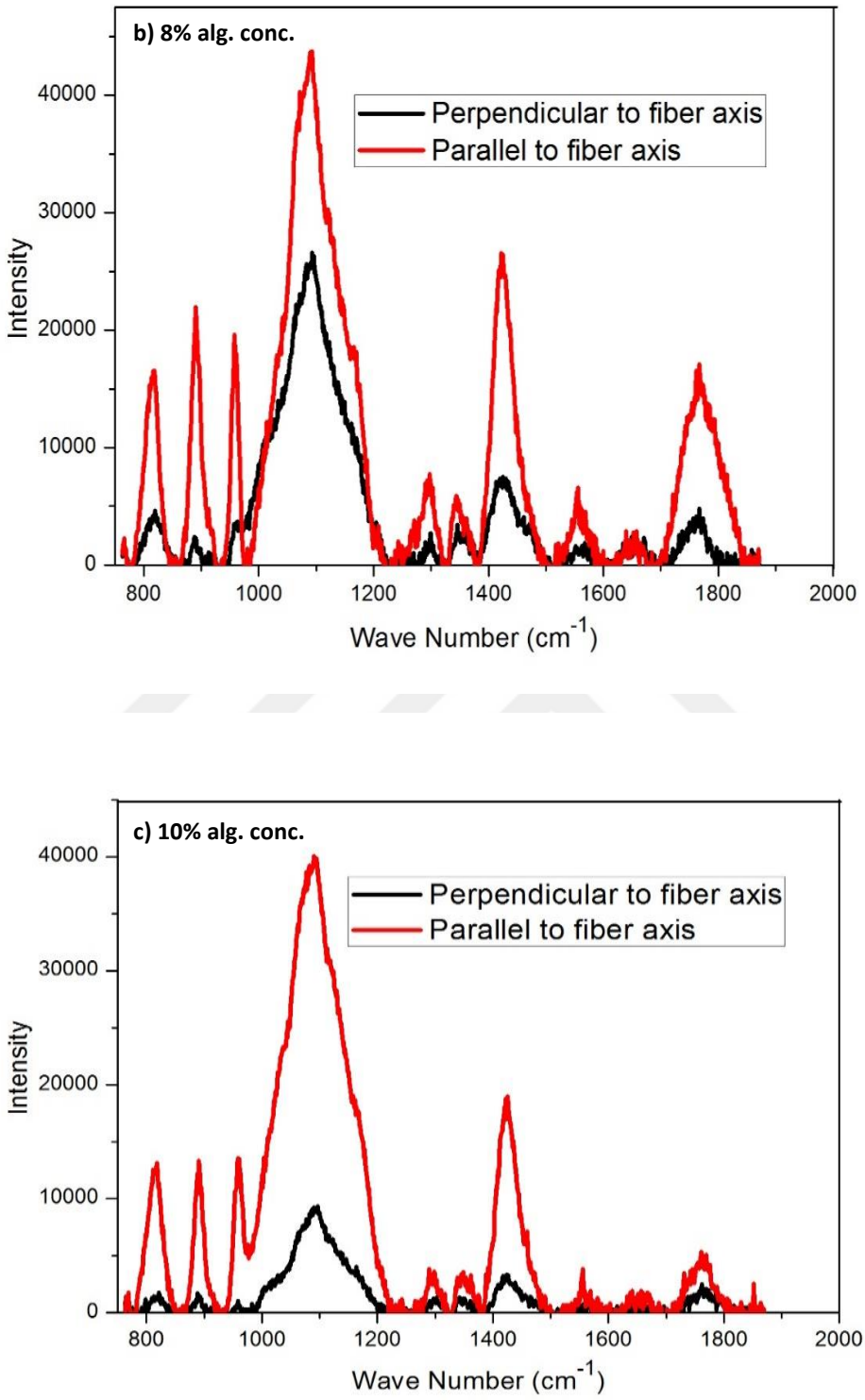

Figure 3.30: Raman spectra of alginate aerogel Fibers (a) 6% (b)8% (c)10% concentration of alginate

The TGA curves for alginate aerogel fibers (Figure 3.31) show that the fibers are thermally stable up to 200 °C. The weight loss from 0 °C to 100 °C is due to moisture while the weight loss from 200 °C to 300 °C is caused by decomposition of the alginate.

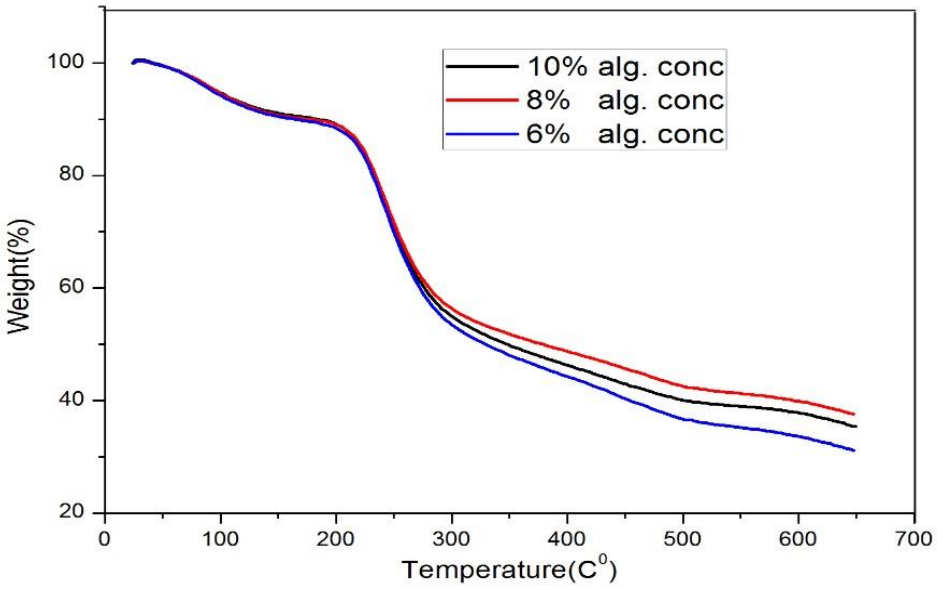

Figure 3.31: TGA curves for alginate aerogel fibers

Chapter 4

CONCLUSIONS AND FUTURE WORK

The aerogel based textiles have become the area of interest for the researchers due to their attractive applications in fields of thermal insulation, erosion control, oil/water absorption, sound absorption and biomedical. In this study, the aerogel textiles were produced and characterized in the form of fibers and composites.

The alginate aerogel was directly synthesized in PET nonwoven fabric by a modified sol-gel procedure. The resulting alginate aerogel-PET nonwoven composite was dust free due to the viscoplastic nature of alginate aerogel between the PET fibers. The thermal diffusivity of the composite was significantly less than the thermal diffusivity of pure PET nonwoven and this results in enhanced thermal insulation as observed by a thermal camera when both fabrics were heated from the bottom.

The thermal diffusivity alginate aerogel-PET nonwoven composite was reduced from 0.233 to 0.142 mm^2/s and thermal resistance is increased from 83.4 to 110.6 mK m^2/W. The tensile strength of the composite was higher than the pure PET nonwoven. The properties can be further improved by increasing the weight fraction of alginate aerogel in the matrix and also by decreasing the thermal conductivity of the alginate aerogel by modifying the synthesis conditions such as the alginate concentration in solution.

The alginate aerogel-PET nonwoven composite has better insulation properties with little weight fraction of aerogel. Furthermore, the alginate aerogel-PET nonwoven composite is non oleophilic, biocompatible and dust free as compared to other available aerogel based composites for thermal insulation application.

The higher weight fraction of alginate aerogel may be caused to achieve the superior thermal properties which can be achieved by increasing the aerogel content or decreasing the fibrous content inside the composite.

The cellulose aerogel cotton nonwoven was produced by immersing the cotton nonwoven inside the solution of cellulose. The cellulose gel was formed at 50 ºC which are later dried supercritically to obtain cellulose aerogel cotton nonwoven composite. The cellulose aerogel was in the form of blocks inside the cotton nonwoven which provided the reinforcement to aerogel network.

The cellulose aerogel cotton nonwoven composite was highly absorbent to wound exudate (fluid). The fluid absorbency of 300 % was recorded by using fluid absorbency standard test method for wound dressings. The silver was loaded over cellulose aerogel cotton nonwoven composite to make it antibacterial. It showed a good antibacterial activity against Escherichia coli bacteria. The XPS results gave the evidence that the silver was present in the form of silver oxide.

Alginate aerogel fibers with good dimensional stability were produced successfully by an extrusion method. It was observed that a minimum 6 wt. % of alginate solution was required for the extrusion of alginate gel fibers. A shrinkage of alginate gel fibers was seen during the gelation. The aerogel fibers have porosities around 80 % and surface areas are around 200 m^2/g.

The concentration of alginate solution has a significant effect on the morphology and mechanical properties of aerogel fibers, so concentration can be selected as a variable to engineer these fibers. By increasing the concentration of alginate, tensile strength was increased whereas the elongation decreased. The aerogel fibers have maximum elongations of 12 % to 15 %. Elastic Modulus of 0.45 MPa is achieved for aerogel fibers. The orientation of aerogel fibers was improved by increasing the concentration of alginate. These alginate aerogel fibers have good stability with porous structure so these may be used to manufacture some novel aerogel based textile products.

These pure aerogel alginate fibers can be blended with conventional fibers like cotton or cellulose. The blending can be done by adding the specific amount of fibers into the solution of alginate. This blending of fibers may improve the mechanical properties of alginate aerogel fibers.

Chapter 5

BIBLIOGRAPHY

[1] M. Matusiak, “Thermal comfort index as a method of assessing the thermal comfort of textile materials,” *Fibres Text. East. Eur.*, vol. 79, no. 2, pp. 45–50, 2010.

[2] S. Ahmad, F. Ahmad, A. Afzal, A. Rasheed, M. Mohsin, and N. Ahmad, “Effect of weave structure on thermo-physiological properties of cotton fabrics,” *Autex Res. J.*, vol. 15, no. 1, pp. 30–34, 2015.

[3] G. Rosace, E. Guido, C. Colleoni, and G. Barigozzi, “Influence of textile structure and silica based finishing on thermal insulation properties of cotton fabrics,” *Int. J. Polym. Sci.*, vol. 2016, 2016.

[4] M. Matusiak and S. Kowalczyk, “Thermal-insulation properties of multilayer textile packages,” *Autex Res. J.*, vol. 14, no. 4, pp. 299–307, 2014.

[5] Y. Li, “The science of clothing comfort,” *Text. Prog.*, vol. 31, no. 1–2, pp. 1–135, 2001.

[6] M. C. Marsh, “The thermal insulating properties of fabrics,” *Proc. Phys. Soc.*, vol. 42, no. 5, pp. 570–588, 1930.

[7] S. Höffele, S. J. Russell, and D. B. Brook, “Light-Weight Nonwoven Thermal Protection Fabrics containing Nanostructured Materials,” *Int. Nonwovens J.*, vol. os-14, no. 4, pp. 1558925005os–14, 2005.

[8] W. E. Morton and J. W. S. Hearle, *Physical Properties of Textile Fibres: Fourth Edition*. 2008.

[9] P. R. Wadje, “Textile - Fibre to fabric processing,” *J. Inst. Eng. (India), Part TX Text. Eng. Div.*, vol. 90, no. AUG., pp. 28–36, 2009.

[10] S. J. Russell, *HandBook of nonwovens*. WOODHEAD PUBLISHING LIMITED.

[11] J. R. Martin and G. E. R. Lamb, "Measurement of Thermal Conductivity of Nonwovens Using a Dynamic Method," *Text. Res. J.*, vol. 57, no. 12, pp. 721–727, 1987.

[12] N. Mao and S. J. Russell, "The Thermal Insulation Properties of Spacer Fabrics with a Mechanically Integrated Wool Fiber Surface," *Text. Res. J.*, vol. 77, no. 12, pp. 914–922, 2007.

[13] D. Das, A. K. Pradhan, R. Chattopadhyay, and S. N. Singh, "Composite nonwovens," *Text. Prog.*, vol. 44, no. 1, pp. 1–84, 2012.

[14] V. G. Yachmenev, D. V. Parikh, and J. A. Calamari, "Thermal insulation properties of biodegradable, cellulosic-based nonwoven composites for automotive application," *J. Ind. Text.*, vol. 31, no. 4, pp. 283–296, 2002.

[15] I. There, "Coherent expanded," vol. 318, no. 1896, 1928.

[16] P. Paraskevopoulou, D. Chriti, G. Raptopoulos, and G. C. Anyfantis, "Synthetic Polymer Aerogels in Particulate Form," 2019.

[17] J. L. Gurav, I. K. Jung, H. H. Park, E. S. Kang, and D. Y. Nadargi, "Silica aerogel: Synthesis and applications," *J. Nanomater.*, vol. 2010, 2010.

[18] B. Ep, J. Christopher, and F. B. Dehn, "Medical use of organic aerogels and biodegradable organic aerogels," EP 0 707 474 B1, 2000.

[19] L. W. Hrubesh, "Aerogel applications," *J. Non. Cryst. Solids*, vol. 225, no. 1–3, pp. 335–342, 1998.

[20] I. Smirnova and P. Gurikov, "Aerogels in Chemical Engineering: Strategies Toward Tailor-Made Aerogels," *Annu. Rev. Chem. Biomol. Eng.*, vol. 8, no. 1, pp. 307–334, 2017.

[21] O. J. Lee, K. H. Lee, T. Jin Yim, S. Young Kim, and K. P. Yoo, "Determination of mesopore size of aerogels from thermal conductivity measurements," *J. Non. Cryst. Solids*, vol. 298, no. 2–3, pp. 287–292, 2002.

[22] K. Daryabeigi, "AIAA 99-1044 Analysis and Testing of High Temperature Fibrous Insulation for Reusable Launch Vehicles 37 th AIAA Aerospace Sciences Meeting and Exhibit," no. c, 1999.

[23] Z. Deng, J. Wang, A. Wu, J. Shen, and B. Zhou, "High strength SiO2 aerogel insulation," *J. Non. Cryst. Solids*, vol. 225, no. 1–3, pp. 101–104, 1998.

[24] T. Rettelbach, J. Säuberlich, S. Korder, and J. Fricke, “Thermal conductivity of silica aerogel powders at temperatures from 10 to 275 K,” *J. Non. Cryst. Solids*, vol. 186, pp. 278–284, 1995.

[25] M. Venkataraman, R. Mishra, D. Jasikova, T. M. Kotresh, and J. Militky, “Thermodynamics of aerogel-treated nonwoven fabrics at subzero temperatures,” *J. Ind. Text.*, vol. 45, no. 3, pp. 387–404, 2015.

[26] J. M. Schultz, K. I. Jensen, and F. H. Kristiansen, “Super insulating aerogel glazing,” *Sol. Energy Mater. Sol. Cells*, vol. 89, no. 2–3, pp. 275–285, 2005.

[27] P. Taylor, “Polymer News : The Polymer Science Monthly General Topics Properties and Uses,” no. October 2014, pp. 10–13, 2006.

[28] W. J. Malfait *et al.*, “Surface Chemistry of Hydrophobic Silica Aerogels,” *Chem. Mater.*, vol. 27, no. 19, pp. 6737–6745, 2015.

[29] T. Woignier, J. Primera, A. Alaoui, P. Etienne, F. Despestis, and S. Calas-Etienne, “Mechanical Properties and Brittle Behavior of Silica Aerogels,” *Gels*, vol. 1, no. 2, pp. 256–275, 2015.

[30] M. Aegerter, N. Leventis, and M. Koebel, *Aerogels handbook (Advances in Sol-Gel Derived Materials and Technologies)*. 2011.

[31] Y. Özbakir and C. Erkey, “Experimental and theoretical investigation of supercritical drying of silica alcogels,” *J. Supercrit. Fluids*, vol. 98, pp. 153–166, 2015.

[32] H. Tamon, T. Kitamura, and M. Okazaki, “Preparation of silica aerogel from TEOS,” *J. Colloid Interface Sci.*, vol. 197, no. 2, pp. 353–359, 1998.

[33] K. Nakanishi, H. Minakuchi, N. Soga, and N. Tanaka, “Double Pore Silica Gel Monolith Applied to Liquid Chromatography,” *J. Sol-Gel Sci. Technol.*, vol. 8, no. 1–3, pp. 547–552, 1997.

[34] X. Chao, S. Jun, and Z. Bin, “Ultralow density silica aerogels prepared with PEDS,” *J. Non. Cryst. Solids*, vol. 355, no. 8, pp. 492–495, 2009.

[35] Z. T. Mazraeh-shahi, A. M. Shoushtari, A. R. Bahramian, and M. Abdouss, “Synthesis, structure and thermal protective behavior of silica aerogel/PET nonwoven fiber composite,” *Fibers Polym.*, vol. 15, no. 10, pp. 2154–2159, 2014.

[36] Z. Zhang *et al.*, “Hydrophobic silica aerogels strengthened with nonwoven

fibers," *J. Macromol. Sci. Part A Pure Appl. Chem.*, vol. 43, no. 11, pp. 1663–1670, 2006.

[37] R. Cited, U. S. P. Documents, and S. Diego, "Flexible aerogel superinsulation and its manufacture," US006068882A, 2000.

[38] S. Devi and S. S. J. Singh, "Use of aerogel in textile and apparel industry," vol. 8, no. 2, pp. 329–332, 2019.

[39] V. Prevolnik, P. K. Zrim, and T. Rijavec, "Textile Technological Properties of Laminated Silica Aerogel Blanket," *Contemp. Mater.*, vol. 1, no. 5, pp. 117–123, 2014.

[40] M. Kisco, "(12) Patent Application Publication (10) Pub . No .: US 2007 / 0199913 A1," vol. 1, no. 19, pp. 2–6, 2007.

[41] K. W. Oh, D. K. Kim, and S. H. Kim, "Ultra-porous flexible PET/Aerogel blanket for sound absorption and thermal insulation," *Fibers Polym.*, vol. 10, no. 5, pp. 731–737, 2009.

[42] A. Shaid, L. Wang, and R. Padhye, "The thermal protection and comfort properties of aerogel and PCM-coated fabric for firefighter garment," *J. Ind. Text.*, vol. 45, no. 4, pp. 611–625, 2016.

[43] M. Venkataraman, R. Mishra, J. Wiener, J. Militky, T. M. Kotresh, and M. Vaclavik, "Novel techniques to analyse thermal performance of aerogel-treated blankets under extreme temperatures," *J. Text. Inst.*, vol. 106, no. 7, pp. 736–747, 2015.

[44] A. Berkefeld, M. Heyer, and B. Milow, "Silica aerogel paper honeycomb composites for thermal insulations," *J. Sol-Gel Sci. Technol.*, vol. 84, no. 3, pp. 486–495, 2017.

[45] E. Se, "Patent_Biodegradable fibers from," vol. 1, no. 12, 2001.

[46] C. A. García-González *et al.*, "An opinion paper on aerogels for biomedical and environmental applications," *Molecules*, vol. 24, no. 9, pp. 1–15, 2019.

[47] K. S. Mikkonen, K. Parikka, A. Ghafar, and M. Tenkanen, "Prospects of polysaccharide aerogels as modern advanced food materials," *Trends Food Sci. Technol.*, vol. 34, no. 2, pp. 124–136, 2013.

[48] P. Gurikov, S. P. Raman, D. Weinrich, M. Fricke, and I. Smirnova, "A novel approach to alginate aerogels: Carbon dioxide induced gelation," *RSC Adv.*, vol.

5, no. 11, pp. 7812–7818, 2015.

[49] M. Martins *et al.*, “Preparation of macroporous alginate-based aerogels for biomedical applications,” *J. Supercrit. Fluids*, vol. 106, 2015.

[50] R. Lin, A. Li, T. Zheng, L. Lu, and Y. Cao, “Hydrophobic and flexible cellulose aerogel as an efficient, green and reusable oil sorbent,” *RSC Adv.*, vol. 5, no. 100, pp. 82027–82033, 2015.

[51] P. Title, A. Publication, D. Article, and T. Orcid, “Flexible nanocellulose-based aerogel with loading of modified UiO-66 as efficient adsorbent for removal of heavy metal ions,” pp. 0–21, 2019.

[52] W. Chen, H. Yu, Q. Li, Y. Liu, and J. Li, “Ultralight and highly flexible aerogels with long cellulose i nanofibers,” *Soft Matter*, vol. 7, no. 21, pp. 10360–10368, 2011.

[53] M. George and T. E. Abraham, “Polyionic hydrocolloids for the intestinal delivery of protein drugs: Alginate and chitosan - a review,” *J. Control. Release*, vol. 114, no. 1, pp. 1–14, 2006.

[54] K. Ganesan *et al.*, “Review on the production of polysaccharide aerogel particles,” *Materials (Basel).*, vol. 11, no. 11, pp. 1–37, 2018.

[55] D. A. Rees and E. J. Welsh, “Secondary and Tertiary Structure of Polysaccharides in Solutions and Gels,” *Angew. Chemie Int. Ed. English*, vol. 16, no. 4, pp. 214–224, 1977.

[56] P. Gurikov, S. P. Raman, D. Weinrich, M. Fricke, and I. Smirnova, “A novel approach to alginate aerogels: Carbon dioxide induced gelation,” *RSC Adv.*, vol. 5, no. 11, pp. 7812–7818, 2015.

[57] R. Rodríguez-Dorado, C. López-Iglesias, C. A. García-González, G. Auriemma, R. P. Aquino, and P. Del Gaudio, “Design of aerogels, cryogels and xerogels of alginate: Effect of molecular weight, gelation conditions and drying method on particles’ micromeritics,” *Molecules*, pp. 4–6, 2019.

[58] M. Alnaief, M. A. Alzaitoun, C. A. García-González, and I. Smirnova, “Preparation of biodegradable nanoporous microspherical aerogel based on alginate,” *Carbohydr. Polym.*, vol. 84, no. 3, pp. 1011–1018, 2011.

[59] L. Y. Long, Y. X. Weng, and Y. Z. Wang, “Cellulose aerogels: Synthesis, applications, and prospects,” *Polymers (Basel).*, vol. 8, no. 6, pp. 1–28, 2018.

[60] A. Zaman, F. Huang, M. Jiang, W. Wei, and Z. Zhou, “Preparation, Properties, and Applications of Natural Cellulosic Aerogels: A Review,” *Energy Built Environ.*, vol. 1, no. 1, pp. 60–76, 2019.

[61] Z. Ulker and C. Erkey, “An emerging platform for drug delivery: Aerogel based systems,” *J. Control. Release*, vol. 177, no. 1, pp. 51–63, 2014.

[62] T. Lu, Q. Li, W. Chen, and H. Yu, “Composite aerogels based on dialdehyde nanocellulose and collagen for potential applications as wound dressing and tissue engineering scaffold,” *Compos. Sci. Technol.*, vol. 94, pp. 132–138, 2014.

[63] F. De Cicco, P. Russo, E. Reverchon, C. A. García-gonzález, R. Patrizia, and P. Del, “Prilling and supercritical drying : A successful duo to produce core-shell polysaccharide aerogel beads for wound healing,” *Carbohydr. Polym.*, vol. 147, pp. 482–489, 2016.

[64] A. Veronovski, Ž. Knez, and Z. Novak, “Preparation of multi-membrane alginate aerogels used for drug delivery,” *J. Supercrit. Fluids*, vol. 79, pp. 209–215, 2013.

[65] J. S. Boateng, K. H. Matthews, H. N. E. Stevens, and G. M. Eccleston, “Wound healing dressings and drug delivery systems: A review,” *J. Pharm. Sci.*, vol. 97, no. 8, pp. 2892–2923, 2008.

[66] S. Enoch and P. Price, “Cellular, molecular and biochemical differences in the pathophysiology of healing between acute wounds, chronic wounds and wounds in the aged,” *World Wide Wounds*, vol. 2005, no. July 2016, 2004.

[67] A. W. C. Chua, Y. C. Khoo, B. K. Tan, K. C. Tan, C. L. Foo, and S. J. Chong, “Skin tissue engineering advances in severe burns: review and therapeutic applications,” *Burn. Trauma*, vol. 4, no. 1, pp. 1–14, 2016.

[68] C. Dowsett and H. Newton, “Wound bed preparation: TIME in practice,” *Wounds Uk*, vol. 1, no. 3, p. 58, 2005.

[69] S. Guo and L. A. DiPietro, “Critical review in oral biology & medicine: Factors affecting wound healing,” *J. Dent. Res.*, vol. 89, no. 3, pp. 219–229, 2010.

[70] M. K. Strecker-McGraw, T. R. Jones, and D. G. Baer, “Soft Tissue Wounds and Principles of Healing,” *Emerg. Med. Clin. North Am.*, vol. 25, no. 1, pp. 1–22, 2007.

[71] H. J. Degreef, “How to heal a wound fast,” *Dermatol. Clin.*, vol. 16, no. 2, pp. 365–375, 1998.

[72] S. Singh, A. Young, and C. E. McNaught, “The physiology of wound healing,” *Surg. (United Kingdom)*, vol. 35, no. 9, pp. 473–477, 2017.

[73] F. Yoshii, Y. Zhanshan, K. Isobe, K. Shinozaki, and K. Makuuchi, “Electron beam crosslinked PEO and PEO/PVA hydrogels for wound dressing,” *Radiat. Phys. Chem.*, vol. 55, no. 2, pp. 133–138, 1999.

[74] D. T. Rovee, “Evolution of wound dressings and their effects on the healing process,” *Clin. Mater.*, vol. 8, no. 3–4, pp. 183–188, 1991.

[75] M. Ramos-e-silva, M. Cristina, and R. D. E. Castro, “New Dressings, Including Tissue-Engineered Living Skin,” no. 1, 1907.

[76] L. Russell, “Understanding physiology of wound healing and how dressings help.,” *Br. J. Nurs.*, vol. 9, no. 1, 2000.

[77] E. W. Brown, “© 1962 Nature Publishing Group,” *Nat. Int. J. Sci.*, vol. 196, pp. 1048–1050, 1962.

[78] K. R. Park and Y. C. Nho, “Synthesis of PVA/PVP hydrogels having two-layer by radiation and their physical properties,” *Radiat. Phys. Chem.*, vol. 67, no. 3–4, pp. 361–365, 2003.

[79] C. C. Wang, C. H. Su, J. P. Chen, and C. C. Chen, “An enhancement on healing effect of wound dressing: Acrylic acid grafted and gamma-polyglutamic acid/chitosan immobilized polypropylene non-woven,” *Mater. Sci. Eng. C*, vol. 29, no. 5, pp. 1715–1724, 2009.

[80] M. Y. Jen and T. L. Hao, “Properties of chitosan containing PP-g-AA-g-NIPAAm bigraft nonwoven fabric for wound dressing,” *J. Memb. Sci.*, vol. 243, no. 1–2, pp. 1–7, 2004.

[81] Timothy Thomson, “Foam composite,” US 7,048,966 B2, 2006.

[82] L. Martin *et al.*, “The release of model macromolecules may be controlled by the hydrophobicity of palmitoyl glycol chitosan hydrogels,” *J. Control. Release*, vol. 80, no. 1–3, pp. 87–100, 2002.

[83] S. Thomas and S. Materials, “A guide to the com position, properties and uses o f hydrocolloid dressings and the com m ercial presentations available,” vol. I, no. 2, pp. 127–130, 1992.

[84] L. L. Lloyd, J. F. Kennedy, P. Methacanon, M. Paterson, and C. J. Knill, “Carbohydrate polymers as wound management aids,” *Carbohydr. Polym.*, vol.

37, no. 3, pp. 315–322, 1998.

[85] C. A. Fleck and R. Simman, “Modern collagen wound dressings: Function and purpose,” *J. Am. Col. Certif. Wound Spec.*, vol. 2, no. 3, pp. 50–54, 2010.

[86] C. J. Doillon and F. H. Silver, “Collagen-based wound dressing: Effects of hyaluronic acid and firponectin on wound healing,” *Biomaterials*, vol. 7, no. 1, pp. 3–8, 1986.

[87] J. P. Chen and W. L. Lee, “Collagen-grafted temperature-responsive nonwoven fabric for wound dressing,” *Appl. Surf. Sci.*, vol. 255, no. 2, pp. 412–415, 2008.

[88] X. Guo, S. Huang, J. Sun, and F. Wang, “Comparison of the Cytotoxicities and Wound Healing Effects of Hyaluronan, Carbomer, and Alginate on Skin Cells in Vitro,” *Adv. Ski. Wound Care*, vol. 28, no. 9, pp. 410–414, 2015.

[89] A. Thomas, K. G. Harding, and K. Moore, “Alginates from wound dressings activate human macrophages to secrete tumour necrosis factor-α,” *Biomaterials*, vol. 21, no. 17, pp. 1797–1802, 2000.

[90] B. Gupta, R. Agarwal, and M. S. Alam, “Textile-based smart wound dressings,” *Indian J. Fibre Text. Res.*, vol. 35, no. 2, pp. 174–187, 2010.

[91] K. Vyas and H. Vasconez, “Wound Healing: Biologics, Skin Substitutes, Biomembranes and Scaffolds,” *Healthcare*, vol. 2, no. 3, pp. 356–400, 2014.

[92] T. Abdelrahman and H. Newton, “Wound dressings: Principles and practice,” *Surgery*, vol. 29, no. 10, pp. 491–495, 2011.

[93] T. R. Hayes and B. Su, “Wound dressings,” *Electrospinning Tissue Regen.*, pp. 317–339, 2011.

[94] J. M. S. F. Rouanet, R. K. Massey, “Aerogel containing blanket,” US007635411B2, 2009.

[95] J. Yan, H. Y. Choi, Y. K. Hong, and Y. G. Jeong, “Thermal insulation performance of cotton and PET-based hybrid fabrics impregnated with Silica Aerogel via a facile Dip-Dry process,” *Fibers Polym.*, vol. 19, no. 4, pp. 854–860, 2018.

[96] M. Venkataraman, R. Mishra, J. Militky, and L. Hes, “Aerogel based nanoporous fibrous materials for thermal insulation,” *Fibers Polym.*, vol. 15, no. 7, pp. 1444–1449, 2014.

[97] Z. Zhang *et al.*, “Hydrophobic silica aerogels strengthened with nonwoven

fibers," *J. Macromol. Sci. Part A Pure Appl. Chem.*, vol. 43, no. 11, pp. 1663–1670, 2006.

[98] M. Venkataraman, R. Mishra, J. Weiner, A. Mazari, J. Militky, and V. K. Arumugam, "Innovative Techniques for Characterization of Nonwoven Insulation Materials Embedded with Aerogel," *World Acad. Sci. Eng. Technol. Int. J. Chem. Mol. Nucl. Mater. Metall. Eng.*, vol. 8, no. 9, pp. 830–837, 2014.

[99] B. Yuan, S. Ding, D. Wang, G. Wang, and H. Li, "Heat insulation properties of silica aerogel/glass fiber composites fabricated by press forming," *Mater. Lett.*, vol. 75, pp. 204–206, 2012.

[100] B. E. Coffman, J. E. Fesmire, S. White, G. Gould, and S. Augustynowicz, "Aerogel blanket insulation materials for cryogenic applications," *AIP Conf. Proc.*, vol. 1218, no. April, pp. 913–920, 2010.

[101] I. Karadagli, B. Schulz, M. Schestakow, B. Milow, T. Gries, and L. Ratke, "Production of porous cellulose aerogel fibers by an extrusion process," *J. Supercrit. Fluids*, vol. 106, pp. 105–114, 2015.

[102] D. Pico, E. Meyer, A. Lüking, B. Milow, and T. Gries, "SILICA-AERO. Production of lightweight silica aerogel fibers for excellent heat insulating application," *Chem. Eng. Trans.*, vol. 60, pp. 91–96, 2017.

[103] G. T. Pico Davide, Schulz Bjorn, Luking Alexander, "Method and device for producing inorganic aerogel fibers," US 20180044187A1, 2018.

[104] K. Y. Lee and D. J. Mooney, "Alginate: Properties and biomedical applications," *Progress in Polymer Science (Oxford)*. 2012.

[105] F. Ahmad, Z. Ulker, and C. Erkey, "A novel composite of alginate aerogel with PET nonwoven with enhanced thermal resistance," *J. Non. Cryst. Solids*, vol. 491, pp. 7–13, Jul. 2018.

[106] I. Frydrych, G. Dziworska, and J. Bilska, "Comparative analysis of the thermal insulation properties of fabrics made of natural and man-made cellulose fibres," *Fibres Text. East. Eur.*, vol. 10, no. 4, pp. 40–44, 2002.

[107] J. Desbrières and V. G. Babak, "Interfacial properties of amphiphilic natural," *Polym.*, vol. 55, no. December 2005, pp. 1177–1183, 2006.

[108] X. He, Y. Liu, H. Li, and H. Li, "Single-stranded structure of alginate and its conformation evolvement after an interaction with calcium ions as revealed by

electron microscopy," *RSC Adv.*, vol. 6, no. 115, pp. 114779–114782, 2016.

[109] S. L. Huang and Y. S. Lin, "The Size Stability of Alginate Beads by Different Ionic Crosslinkers," *Adv. Mater. Sci. Eng.*, vol. 2017, 2017.

[110] P. Gurikov and I. Smirnova, "Non-Conventional Methods for Gelation of Alginate," *Gels*, vol. 4, no. 1, p. 14, 2018.

[111] M. A. Kamaruddin, M. S. Yuso, and H. A. Aziz, "Preparation and characterization of alginate beads by drop weight," *Int. J. Technol.*, vol. 5, no. 2, pp. 121–132, 2014.